

Real-Time Electrochemical Assessment of Soil Health Through EAB Formation and the Development of a Stimulus-Responsive Remediation of Microbial Soil Degradation

Siyeong Park

Shanghai American School Puxi Campus

*Corresponding author: Siyeong Park, Shanghai American School Puxi Campus.

Submitted: 02 August 2025 Accepted: 07 August 2025 Published: 11 August 2025

doi <https://doi.org/10.63620/MKWJSNR.2025.1042>

Citation: Park, S. (2025). Real-Time Electrochemical Assessment of Soil Health Through EAB Formation and the Development of a Stimulus-Responsive Remediation of Microbial Soil Degradation. *Wor Jour of Sens Net Res*, 2(4), 01-27.

Abstract

The objective of this study is to establish a real-time bio electrochemical assessment of microbial soil health through EAB formation, due to the flaws of conventional soil health evaluation methods in the status quo. This study employs a three-electrode system to run CA and CV trials in the soil environment in healthy and unhealthy soil categories. In the healthy soil category, the trials have effectively validated that the CA and CV trials were able to effectively represent the soil's health in real-time, while EAB formation and maturation synergistically enhanced soil health microbiologically through confirmation from CA and CV trials. In contrast, the unhealthy soil category which was simulated by killing the microorganisms through applying extreme heat via vertical pressure steam sterilizer, has displayed a weak EAB formation as well as real-time soil health, which was also confirmed through CA and CV trials. However, EAB was not utilized effectively as the soil barely had any microorganisms available to form communities which could lead to EAB formation. As a result, this research proposes an engineering extension to leverage the findings and add supplemental technologies in pursuit of not only assessing microbial soil health real time but also actively remediating soil. To achieve such agenda, the engineering extension involved developing an inoculation system involving electrothermal wax cartridge and alginate beads enclosed with biodegradable outer mesh, to release micronutrients and microbial consortia based on decisions from AI trained using the CA and CV trials of this study. Furthermore, a sample website was built to run sample CA and CV trials, where users could upload their own CA or CV trials to receive analysis/recommendation from the trained AI model, and receive recommendations on further actions on the CA and CV trial simulation from the trained AI model. Overall, this study brings value to the realms of this research as it enables in-situ, non-destructive methods of soil biosensing as well as soil remediation, without affecting soil acidification issues, but enhancing carbon sequestration capacities of the soil. Therefore, when plants are planted in healthy soil, the aforementioned factors will indirectly enable the optimal efficiency in photosynthesis, contributing to climate change mitigation. A potential limitation to tackle is implementing the unpredictable nature of soil into this bio electrochemical approach, in order to optimize it for a more effective real-world application.

Keywords: Electrochemically Active Biofilms, Soil Health Assessment, Cyclic Voltammetry, Chronoamperometry, Microbial Fuel Cells, Extracellular Electron Transfer

Abbreviations

CA: Chronoamperometry

EAB: Electrochemically Active Biofilm

MFC: Microbial Fuel Cell

CV: Cyclic Voltammetry

EAM: Electrochemically Active Microorganisms

BES: Bio electrochemical Systems

EPS: Extracellular Polymeric Substances

EET: Extracellular Electron Transfer

AI: Artificial Intelligence

Introduction

Having double the atmosphere carbon storage capacity (~750 Pg C) and triple the biosphere carbon storage capacity (~560 Pg C), soils possess a carbon storage capacity of 1500 Pg of soil organic carbon in 1m depth alone; furthermore, soil is globally the second largest carbon sink, after oceans (~38,000 Pg C) [1, 2]. It is important to note that land degradation - driven from deforestation, wildfire, drought, and post mining areas - gave rise to problems including microbial extinction, soil structure collapse, and loss of carbon sequestration capacity in soil; especially, 133 billion tonnes of carbon has been released from soil since humanity began agriculture, while one third of it could have been deposited back into soil if critical land degradation caused by human actions and industrialization didn't take place [3-6]. Still, agricultural expansion drives nearly 90% of global deforestation, but soil quality deteriorates in deforested areas, ironically reducing both yields (~30%) and rainfall [7, 8]. These statistics directly manifest the significant problems land degradation poses towards the environment and the society. Yet, conventional soil health evaluation depends heavily on physico-chemical indicators including pH, organic matter content, and texture. Firstly, these methods are often labor-intensive, destructive, non-real-time, and spatially sparse. Moreover, while these parameters provide useful superficial data, they fail to capture the dynamic, functional, and real-time aspects of soil biogeochemistry; they especially fail to capture the state of the microbial system, which is crucial in soil's nutrient cycling, carbon sequestration, and structural stability.

Critically, microbial vitality and redox balance - the important engines of soil functionality - are inexplicable in aforementioned conventional soil health assessment methods. There are no standardized methods of evaluating activity of electroactive microbes, EET capacity, or redox-mediated feedback loops that supervise soil's biological self-repair mechanisms. Thus, during early phases of soil degradation, when intervention is still viable, it is extremely difficult to act to intervene. When physical symptoms such as aridness and erosion is displayed, the microbial infrastructure is often already collapsed, as well as the difficulty level of soil recovery gets exponentially harder and expensive.

Biofilm is a community of microorganisms that adheres to inert or living surface by a self-produced polymeric matrix; they are ubiquitous in natural ecosystems, and they significantly boost the survival of its incorporated microorganisms by rendering them 1000 times more resistant to diverse types of pressure [9, 10]. In other words, biofilms are specifically created to protect bacteria collectively from the external environment, exploiting its persistence and functionality for survival [11, 12]. Biofilms are capable of promoting soil nutrient cycling, thus increasing soil fertility and preventing soil degradation [13]. EAB, a type of biofilm which this research primarily focuses on, is formed on electrodes of MFCs when electroactive microorganisms transfer electrons with it [14]. Through CA, literature like has confirmed that its currents could be employed to understand the trends of biofilm health, EPS maturation, and EET enhancement. Overall, EAB has various merits of solving the critical soil degradation

problem and soil health evaluation [15].

In addition to EAB formation, this study employs EET driven redox reactions. Redox reactions are referred to as oxidation-reduction reactions, where oxidation is carbon in organic molecules which lose electrons, while reduction is molecular oxygen which gain electrons. Despite the significance of redox reactions where it influences nutrient uptake and mobility, plant growth, microbial community, and soil structure, this reaction is considerably low and is inefficient on soil health in the natural state [16]. Through inserting a working electrode to artificially enhance electron transfers involved in redox reactions, promoting EAB formation, applying controlled potentials to stimulate redox reactions using CV and CA, and measuring such electrochemical treatment, this study aims to take advantage of redox reaction for soil health and recovery to amplify, control, and quantify redox reactions.

This study approaches direct, real-time, continuous, non-invasive soil health assessment through the means of electrochemical techniques; additionally this study extends the line of other papers - which suggests that it indicates soil health via bio electrochemical signals like CV and CA [17]. This system will add on activating a BES to mobilize dormant nutrients, monitoring redox ability and biofilm function, and establishing a closed loop that involves electrochemical signals triggering simulation protocols.

This study hypothesizes the following: introducing a one-time glucose input and rendering three electrode systems implemented on soil samples (healthy and unhealthy soil category) will stimulate the formation of EABs on a carbon felt working electrode, outputting an effective representation of soil health. This microbial activity will be reflected in increased CA current and sharper redox peaks with reduced ΔE in CV. These electrochemical responses will serve as real-time, label-free indicators of microbial recovery and soil biotic regeneration, demonstrating EAB-based sensing as a novel approach for monitoring soil health. Through the findings of the research, the potential of this study could extend towards active soil remediation and carbon sequestration, meaningfully contributing towards climate change mitigation.

Materials and Methods

There are two categories of soil incorporated in this research: healthy and unhealthy soil category. The soil samples were collected from Jilin University Campus Garden. The collected soil was employed for the healthy soil category of this research, and 30mL of 0.5M glucose was added once to both categories to fuel microbial growth, metabolism, and soil respiration [18, 19]. It was added only once as adding more would provoke overgrowth, thus it would not align with realistic settings of nutrient pulse that soil typically experiences in the natural ecosystem. The unhealthy soil category of this experiment was simulated by putting the collected healthy soil into the Vertical Pressure Steam Sterilizer at 121°C for 1 hour to thermally kill microorganisms and minerals that the soil contained.



Figure 1: Healthy Soil Placed in Vertical Steam Pressure Sterilizer to kill Microbial Communities

In this research, a three-electrode system was employed, and all electrochemical trials including CV and CA were performed on a Chenhua CHI660E electrochemical workstation. For the working electrodes, a 16cm^2 (4X4) square electrode was designed using carbon felt; for a counter electrode, platinum wire electrode was used; and for the reference electrode, a saturated

calomel electrode was used. Carbon felt was used as a working electrode because they are traditionally used in MFC practical applications [20]. The working electrode was placed 2cm below the surface level of the soil for both healthy and unhealthy soil categories.



Figure 2: Carbon Felt Working Electrode Setup (4X4)



Figure 3: Bird's eye view of three Electrode System (Working, Reference, counter Electrode set up)

The following is the parameters of every CA trials, for both healthy and unhealthy soils:

Initial Voltage (V): 0.2

Sample Interval (sec): 0.1

Quiet Time (sec): 0

Sensitivity (A/V): 1.e-003

The fixed initial voltage of 0.2V with a 0.1 second of time interval ensured moderate promotion of electron transfer to be captured by real-time current response behavior. The sensitivity of 1.e-003 is the standard for MFC applications, where noise suppression and current change detection is mostly balanced.

The following is the parameters of every CV trials, for both healthy and unhealthy soils:

Initial Voltage (V): -0.8

Maximum Voltage (V): 0.8

Minimum Voltage (V): -0.8

Final Voltage (V): -0.8

Initial Scan Polarity: Positive

Scan Rate (V/s): 0.1

Sweep Segments: 6

Sample Interval (V): 0.001

Quiet Time (sec): 2

Sensitivity (A/V): 1.e-003

A potential sweep of [-0.8, 0.8] is commonly used in studies in the topic of redox-active soil constituents shown by the work of Li et al. and Rimboud et al. Multiple sweep segments of six cycles are commonly employed in evaluation of biofilm electrochemical stability or hysteresis [21, 22]. The quiet time of 2 seconds is recommended in CV protocols, which facilitates noise prevention from porous electrodes or soil matrix [23].



Figure 4: Bird's eye view of Experiment set up with Parafilm Applied



Figure 5: Side view of the Overall Experiment set up

Bemis Parafilm M was applied on top of the structure to reduce evaporation of water for both healthy and unhealthy categories, thus preventing water/moist loss of the soil (noting that the parafilm was partially not applied for areas around the three electrodes for their connection). Following the findings of this study,

soil samples were collected within the depth range of 0cm~16cm - where the relationship between the actual soil condition and relevant measurements (including pH) has the highest accuracy of properly representing soil conditions [24]. The pH of soil and distilled water mixture - where distilled water does not influ-

ence the pH of the soil samples - was measured using a manual LY101 soil pH meter. Thus, a parallax error of ± 0.1 pH could be assumed for the measured values in this study.

Results

Multiple CA and CV trials were executed for both healthy and unhealthy soil categories. Approximately 7 days were spent on both CA and CV trials for the healthy soil category, while about 6 days were spent for the unhealthy soil category. For certain CA trials that were held on relatively small amounts of time (below 5000 seconds) were considered insignificant to include in the trials since they would not be able to fully capture the relationship between the current and time elapsed on the soil.

CA Trials

Chronoamperometry (CA) is an electrochemical analytical technique that measures electric current over time when a fixed voltage is applied to a system. The general purpose of running CA trials is to study the kinetics of chemical reactions, diffusion processes, and absorption. In this particular experiment, CA trials are utilized to not only monitor the health of the soil in real time in a quantitative manner but also to actively stimulate biofilm formation - specifically, electrochemically active biofilms (EAB).

Healthy Soil Category

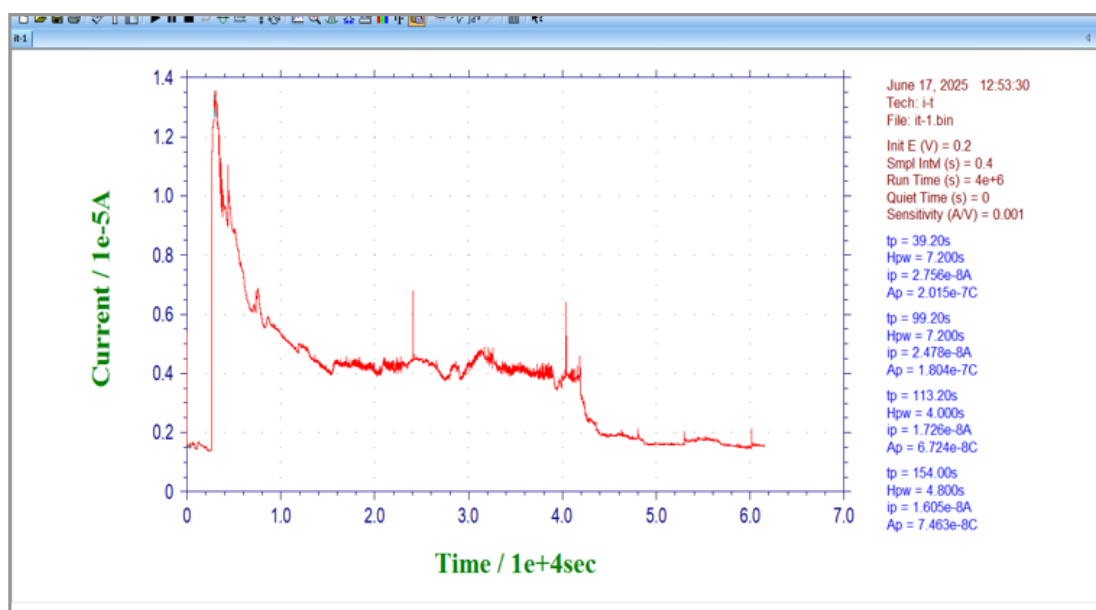


Figure 6: Trial 1

Since distilled water was added at the start of this research to ensure conductivity, there is an extreme boost of the current at the start of this CA trial. An exponential decay pattern was observed

in this trial, and the current initially stabilizes around 4×10^{-6} A then decreases to stabilize around 2×10^{-6} A.

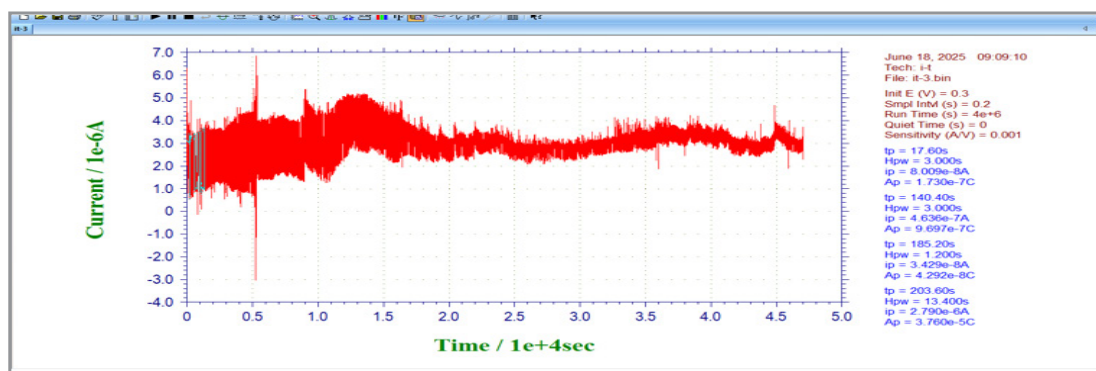


Figure 7: Trial 2

The exceedingly thick line shown in this trial is attributed to high-frequency electrochemical fluctuations; the primary reason for the dynamic biofilm restructuring and heterogeneous redox conditions within the soil matrix. Considering that this trial was run approximately 20 hours after the previous trial, where water and glucose input occurred, such fluctuations are likely due to the increased redox reactions as carbon in glucose gets oxidized (loses electron) and oxygen molecule is reduced (gains electron). While it is also possible to interpret that such thick

lines are attributed to a sudden substrate uptake after maturation of EAB, thus causing a burst of electron release, it is impractical to interpret in such way as this trial was run approximately around the 48-hour timeframe since the experiment has started, thus the chance of biofilm formation is not realistic. In fact, in the CA trials of this soil category, there are other trials (trial 4 and 5) which strikingly display where EAB is formed. Thus, it is rather realistic to interpret this thick line as a fluctuation from redox reactions.

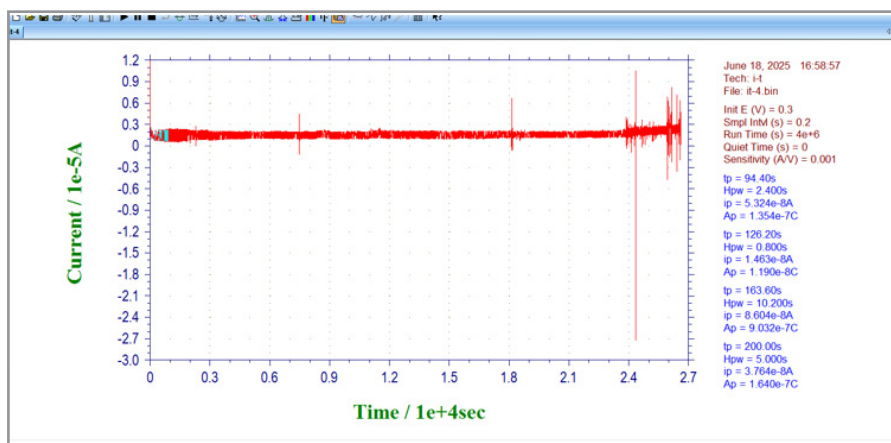


Figure 8: Trial 3

Trial 3 does not indicate striking changes in the current. It remains stable while there are slight vertical shifts which are predicted to be caused by external factors such as noise. Trial

3 shows that the soil environment has adapted to the chemical additions, which is glucose and water, and entered a phase of stabilized current.

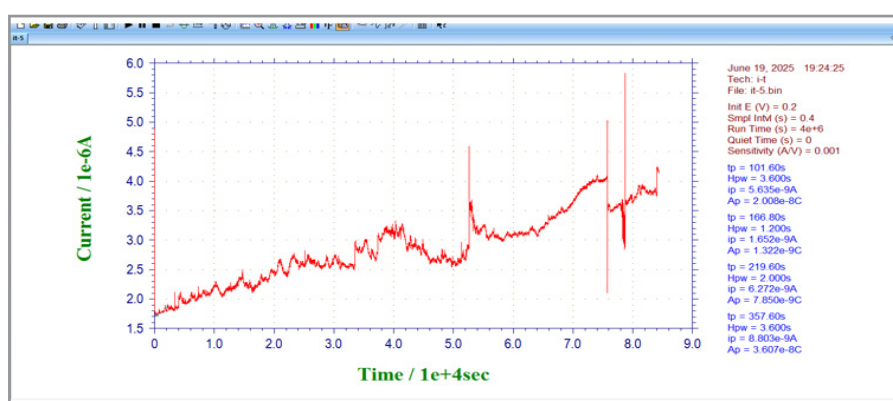


Figure 9: Trial 4

A peculiar element shown in trial 4 is that there is a secondary rise of current, which differs from prior CA trials that were often stabilized at a certain point or remained uniform for the full trial.

This aligns with the discovery among previous research, where a secondary current rise is an indication of biofilm formation on electrode surface [25].

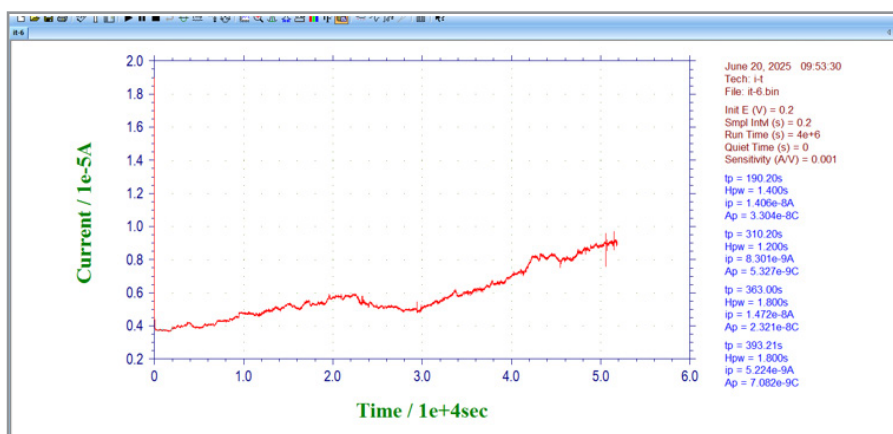


Figure 10: Trial 5

Trial 5 also indicates a subtle secondary rise in its CA graph. As mentioned on trial 4, trial 5 also indicates biofilm growth on the electrode surface. A difference to note in trial 5 is that its current is approximately twice as high as trial 4, suggesting increased metabolic activity, where the redox reactions are occurring

more effectively, thus additionally suggesting improved electron transfer efficiency as it is higher than the previous CA trial. As a result, biofilms thicken as a populated community forms with electroactive microorganisms, which also matures the biofilm.

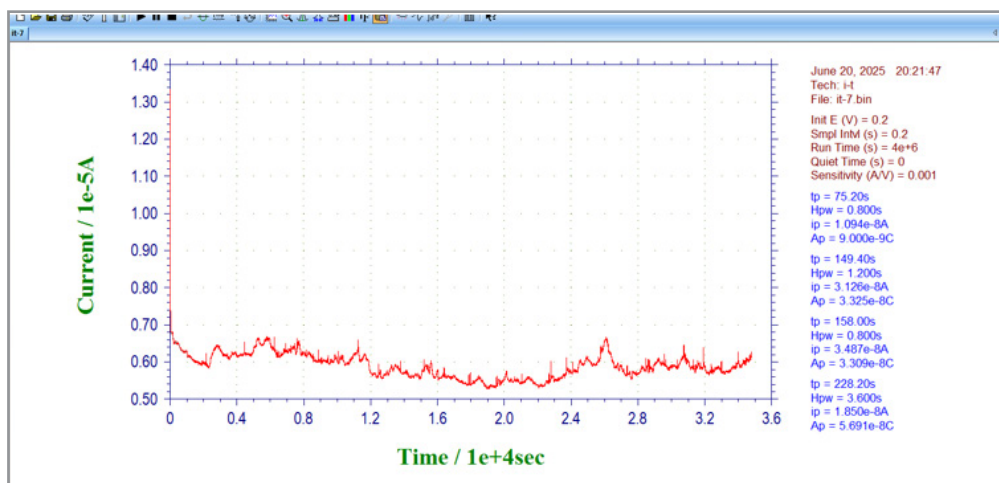


Figure 11: Trial 6

Trial 6 displays a more stabilized graph compared to trial 4 and 5 where EAB was formed, but still involves minor fluctuation in current. This suggests that the biofilm is becoming more consistent, stabilized, and mature.

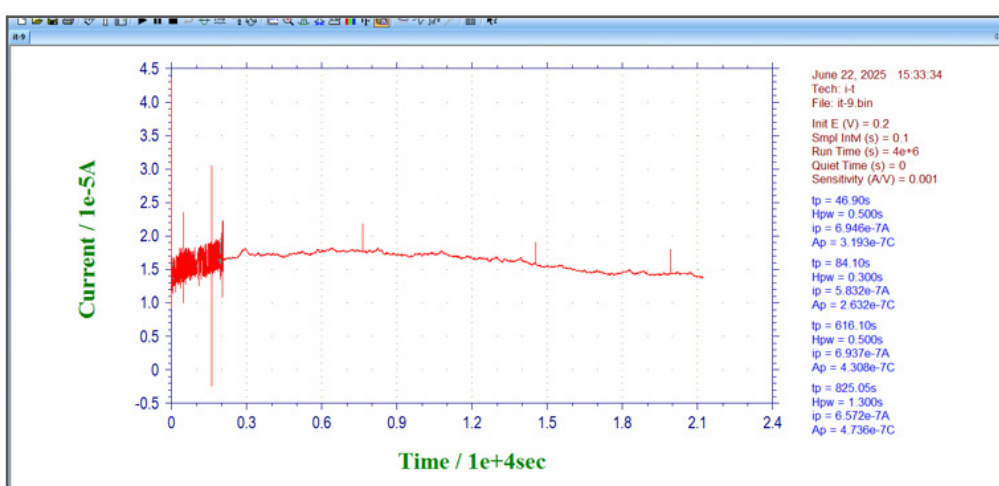


Figure 12: Trial 7

Trial 7 extends the prediction of biofilm maturation and optimization aforementioned in trial 6. Despite the initial fluctuation from [0, 0.3E04] interval, which seems to be due to interference or noise at the start of the experiment, the line overall is highly stable with occasional slight peaks. As the graph became more stabilized in this trial, this represents that the electron transfer pathway of the biofilm has been fully established, enabling efficient electron transport. Furthermore, it is also possible to infer that the microbial community structure in conjunction with metabolic activity have become more consistent, overall demonstrating biofilm maturation.

This stabilization occurs due to biofilm's stabilization mechanism: it initially forms a dense biofilm matrix where EPS and conductive networks start to stabilize, and after a balance has been reached as microbial competition subsides, it leads to a stable population of electroactive microorganisms. Finally, the thickness of the biofilm reaches its optimal level, balancing nutrient diffusion with electron transport efficiency. Trial 7 primarily follows the idea of such a mechanism.

steady increase in anodic current density, rising from an initial baseline of approximately $0.125\mu\text{A}/\text{cm}^2$ to a stabilized density at around $0.9375\mu\text{A}/\text{cm}^2$ by the final trial, indicating progressive EAB formation in conjunction with development on carbon felt surfaces. Furthermore, it has displayed formation of EAB as well as its process of stabilization and maturing, eventually reaching the balance to gain the optimal version of EAB. This essentially achieves two objectives of this study: to establish a reliable soil health monitoring system, and remediate soil through formation and maturation of EAB. The formation of biofilm demonstrates the presence of microbes and its biological activation in the soil. As biofilm stabilizes, it outputs a consistent current as shown as trial 7. This correlates with microbial activity and soil electrochemical properties, serving as a biosensor to monitor soil health real-time. Furthermore, as biofilm matures, it restores soil structure, biogeochemical cycles, and pollutant breakdown capabilities. As a result, mature EABs become bio-stimulatory systems to accelerate soil remediation by effectively activating beneficial microbial functions.

Unhealthy Soil Category

Overall, the CA trials of the healthy soil category displayed a

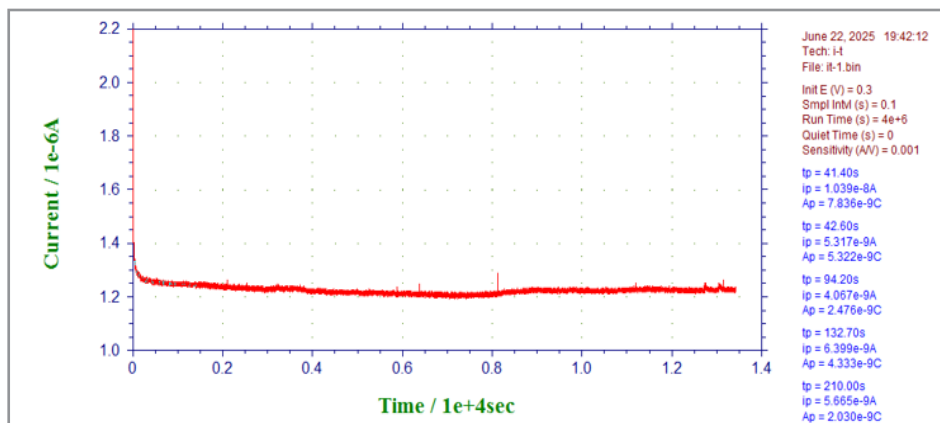


Figure 13: Trial 1

Despite that glucose and distilled water was added into the soil environment, trial 1 indicates no significant changes.

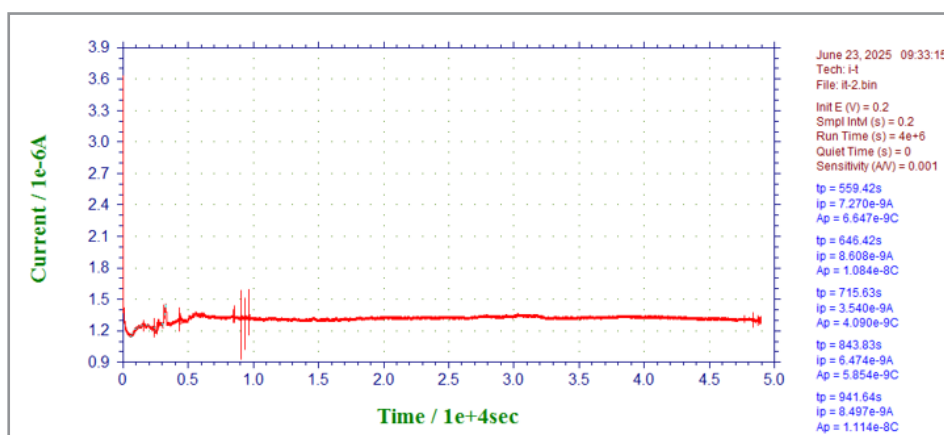


Figure 14: Trial 2

There is a slight secondary rise of current in trial 2, between the interval of $[0, 5E03]$. This time interval is approximately half of the time spent running trial 1 (the overall time spent on this trial was 49269.8 seconds, while 13419.9 seconds were spent on the

previous trial). Considering that, the secondary rise indicated in this trial is significant and can be attributed to the EAB formation on the electrode surface.

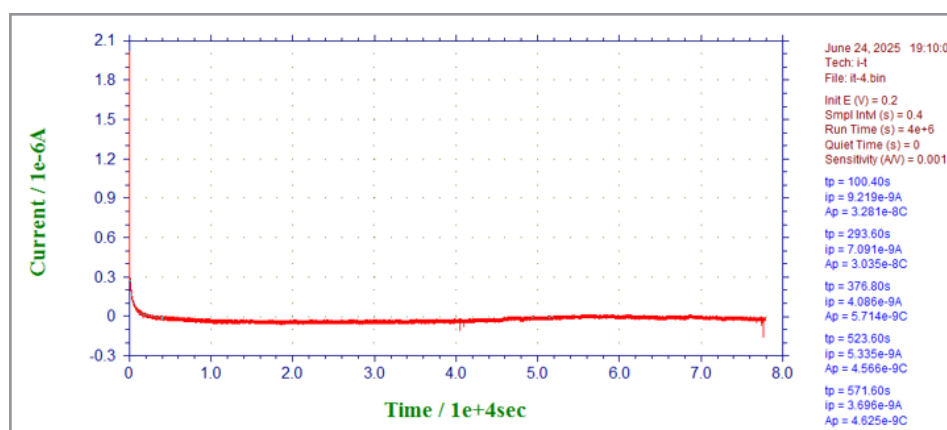


Figure 15: Trial 3

Trial 3 indicates stabilized current; one difference from trial 3 and its previous one is that the initial current has dropped from about $1.5E-06A$ to about $3E-07A$. In regards to the CV trials, it

strongly suggests that EAB was formed on this and the subsequent trial.

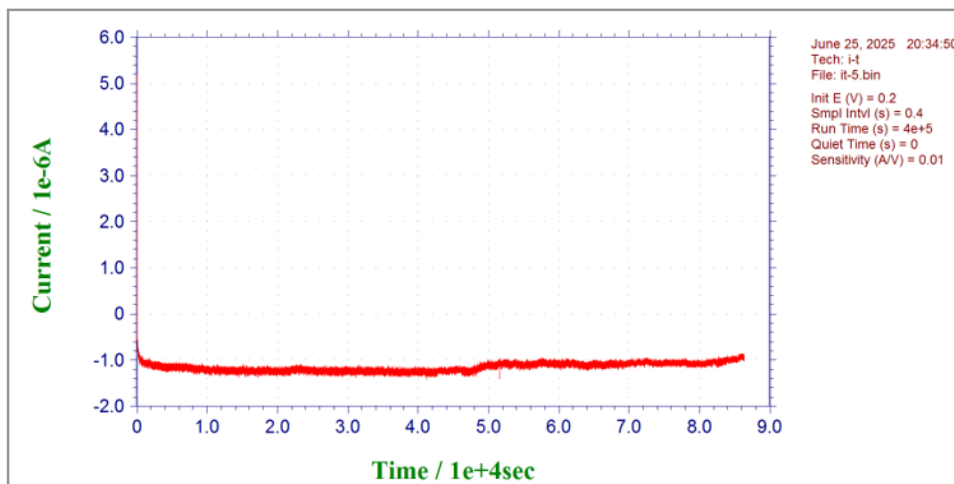


Figure 16: Trial 4

The line becomes thicker from this trial and maintains a similar thickness for successive trials. This implies that the EAB was

formed around this trial (or possibly trial 3) then progressed with its maturing process.

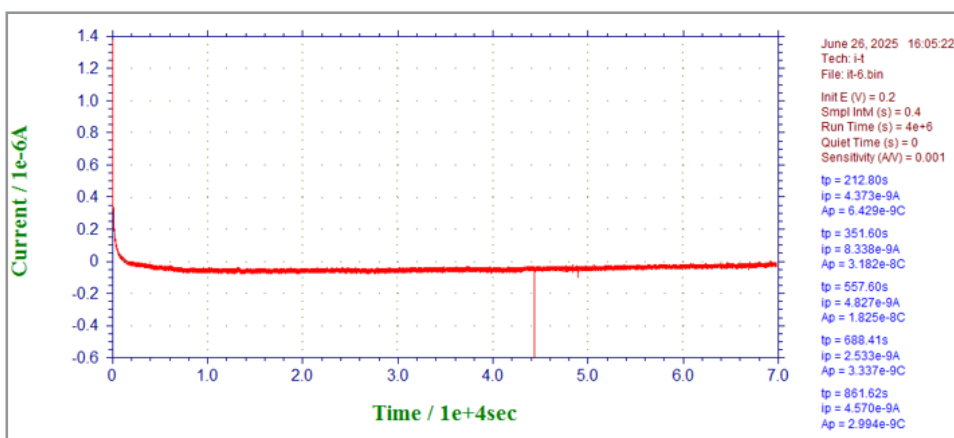


Figure 17: Trial 5

There are no significant changes in trial 6 except the sudden drop of current around 4.4E04 seconds. The drop is due to external noises, and can be considered insignificant for this research.

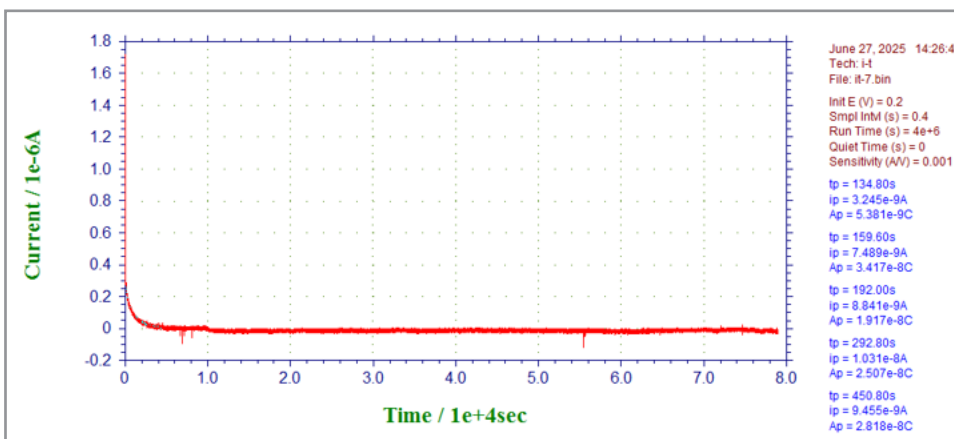


Figure 18: Trial 6

There are no significant changes in this trial as well apart from slight current drops, which can be attributed to external noises.

During the unhealthy soil category CA trials, starting from trial 3, the final current started to become negative - which means that the electrons are flowing into the working electrode instead

of being dispersed. Seeing as the final current for CA trial 1 and 2 was positive, this behaviour is likely due to initial lack of oxidizable microbial species near the working electrode, while they become scarce as the leftover species (including glucose) are consumed, the oxidation reaction eventually slowed down or stopped. Subsequently, a reduction reaction onset, which is why

the final current is negative from the third CA trial.

Compared to the CA trials of the healthy soil category, the CA trials of the unhealthy soil category do not display relatively striking changes through the graphs. This ambivalently shows the strengths and the flaws of this experiment. Due to the fact that most of the microorganisms die from applying extremely high temperature on the soil through vertical pressure steam sterilizer, it leaves only a bare minimum of (or even none) microbial communities that can develop to form weak EAB. Despite that glucose and water was added, where it could provide a limited amount of organic materials, its decomposition would be considerably slow compared to the existing microorganisms and its community in healthy soils. Even under ideal conditions, where the EAB was formed, which was slightly implied through the CA graphs, its maturing period is prolonged compared to the maturing period displayed through the healthy soil category. Overall, this ambivalently shows the strength of this CA trial directly detecting health of the soil real time, while the flaw that it is limited to remediate the soil with electrochemical techniques itself through the current techniques - it is necessary to add other organic nutrients that does not take soil prolonged period of time to decompose to acquire the type of microbial community available in healthy soils. Both the strength and the flaw displayed through the CA trials of unhealthy soil category can be consid-

ered for the future applications and directions of this research.

CV Trials

Cyclic voltammetry (CV) is a potentiodynamic electrochemical technique widely used for studying electron transfer mechanisms that occur inside EABs. CV is performed by cycling the potential (in other words, linear sweep in both directions at the same rate) of the working electrode between two selected values measuring the resulting current. A unique advantage of CV compared to other similar techniques is that it maintains the material in its original form, which is beneficial for this research as the working electrode surface uniformity is crucial for consistency in EAB formation and fairness among healthy and unhealthy soil categories. Furthermore, for real world application conditions, it is beneficial as it could be easily employed without altering the form of the initial soil conditions. In addition, as CV trials are used extensively to understand redox behaviours, this aligns adequately with this study (Cyclic Voltammetry - an Overview | ScienceDirect Topics, n.d.). This section is more focused on the individual CV trials rather than its comparison and development along with its progression. The comparison will be focused on the section of overlaying 2 consecutive CV graphs subsequently.

Healthy Soil Category

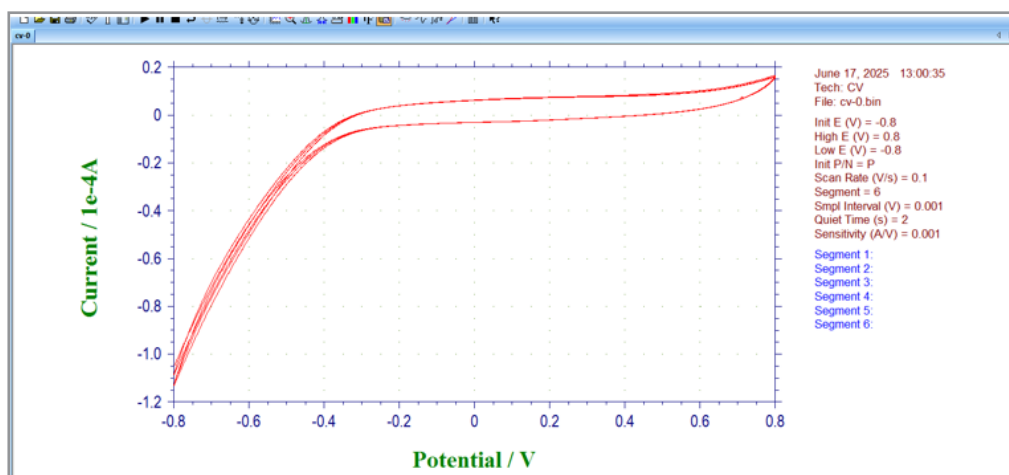


Figure 19: Trial 0 (Before adding Glucose)

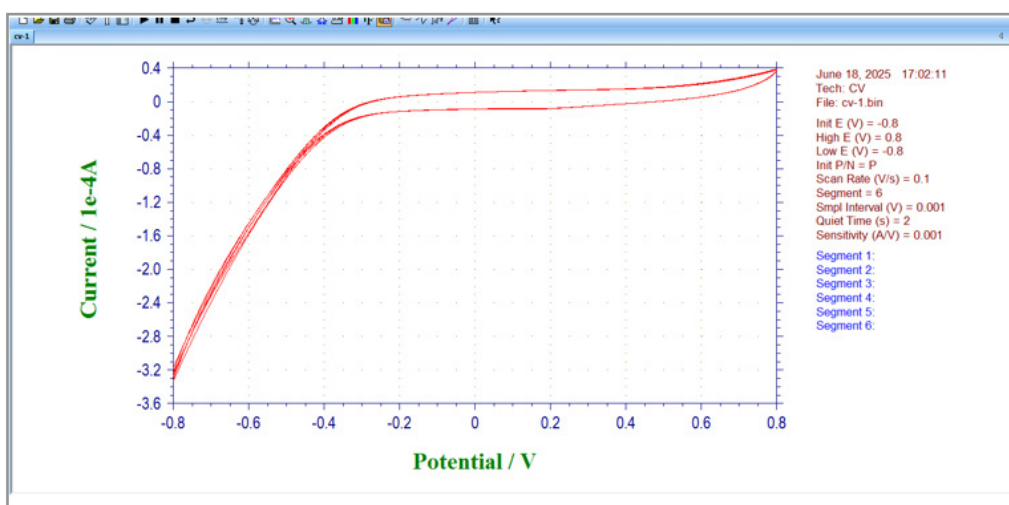


Figure 20: Trial 1 (After applying 0.5M 30mL of Glucose)

A striking decrease in initial current from $-1.1\text{E-}04$ to $-3.2\text{E-}04$ A occurred after applying glucose to the system. This indicates redox silence or microbial activity. Since this trial was run directly

after glucose was added to the system, the chemical bonds of the glucose have not been organically nor electrochemically decomposed in this period. Thus, the initial current suddenly drops.

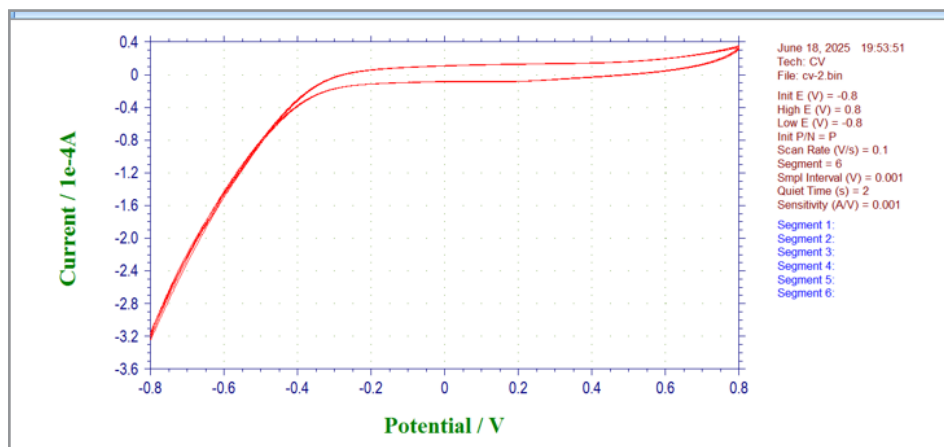


Figure 21: Trial 2

The initial current from trial 1 is maintained in this trial.

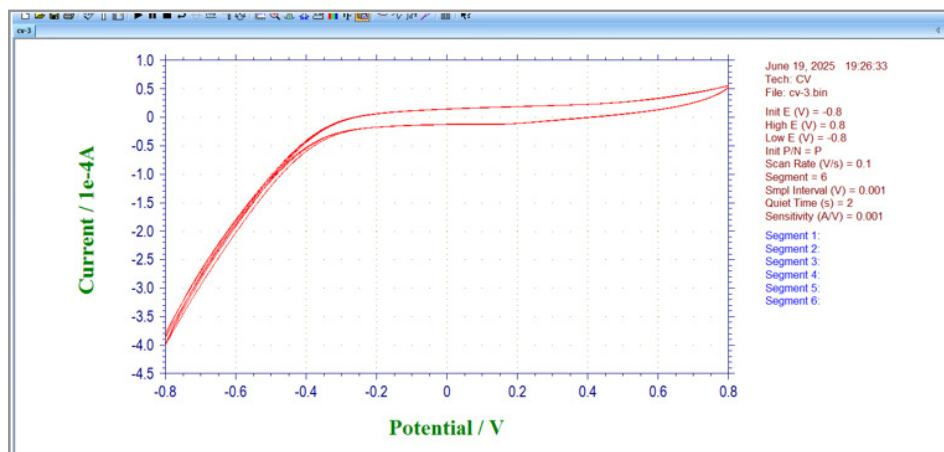


Figure 22: Trial 3

The initial current suddenly drops to $-4.0\text{E-}04$ from $-3.2\text{E-}04$ A once again in this trial. This indicates that the electrode surface is becoming passivated, as biofilm gets formed and attached to

the working electrode surface. This aligns with the results shown from the similar timeframe of the CA trials (refer to CA trial 4, healthy category).

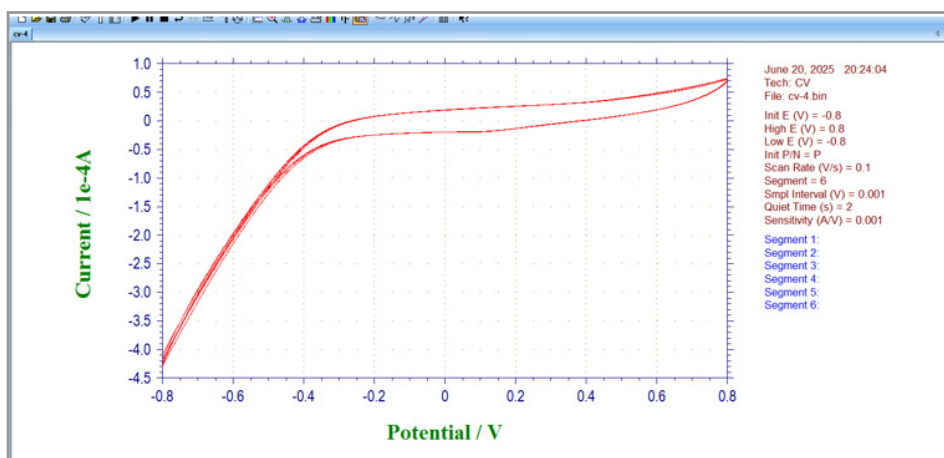


Figure 23: Trial 4

The initial current is maintained from trial 3. It is possible to infer that it is going through EAB maturation processes in conjunction with system stabilization, and once the biofilm becomes mature and the system reaches for stabilization, there would be

an additional expected drop in initial current. This is because those factors will make the working electrode be covered up with biofilm, getting into the way of electron transfer between the working electrode and the soil.

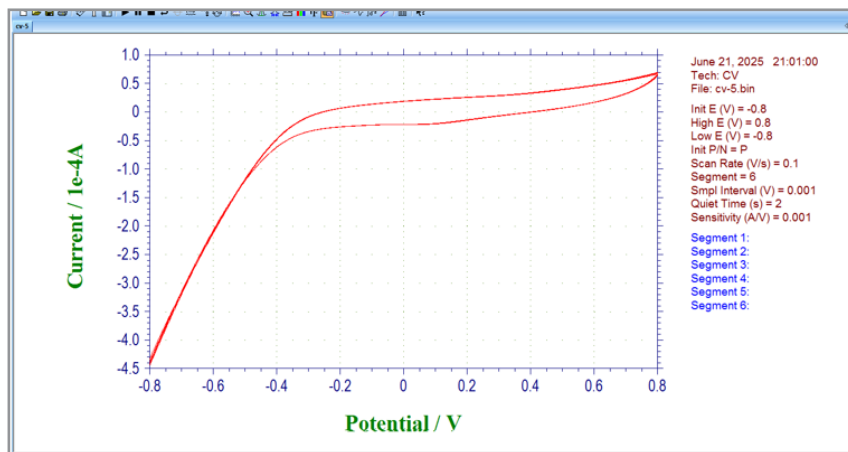


Figure 24: Trial 5

The initial current drops to -5.0×10^{-4} A from -4.4×10^{-4} A. This further demonstrates that the soil is continuously going through biofilm maturation and system stabilization.

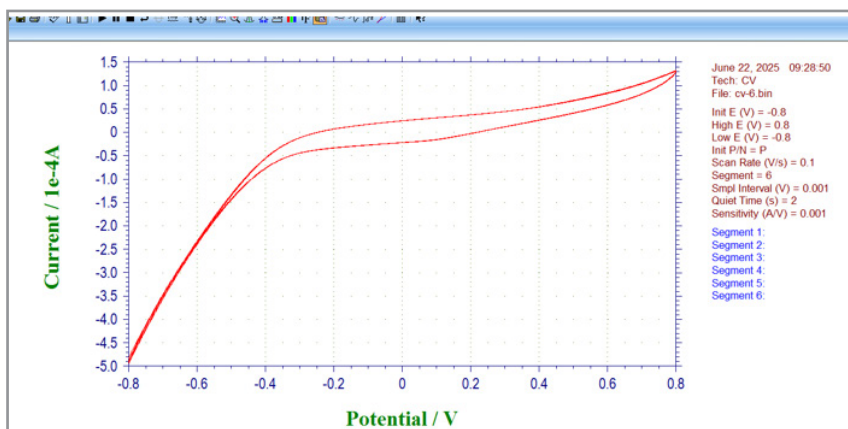


Figure 25: Trial 6

The initial Current is Maintained from Trial 6.

Unhealthy Soil Category

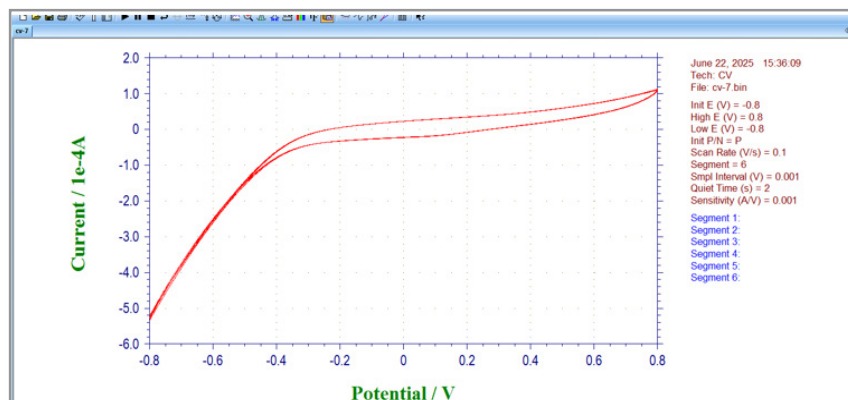


Figure 26: Trial 7

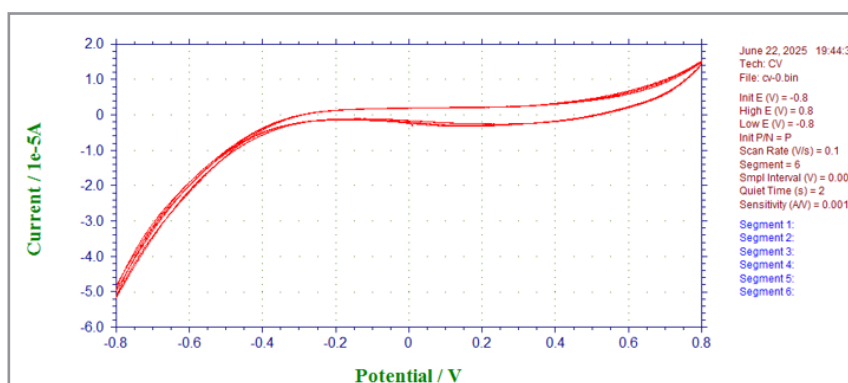


Figure 27: Trial 0 (Before adding Glucose)

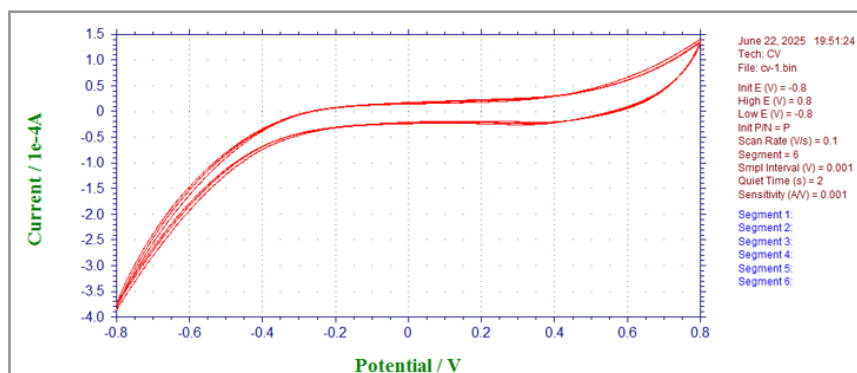


Figure 28: Trial 1 (After adding 0.5M 30mL of Glucose)

The initial current drops significantly from -5.0×10^{-5} to -3.7×10^{-4} A after glucose is added to the system. Similar to the CV trials of

the healthy soil category, this indicates redox silence or microbial activity as glucose is not fully decomposed yet.

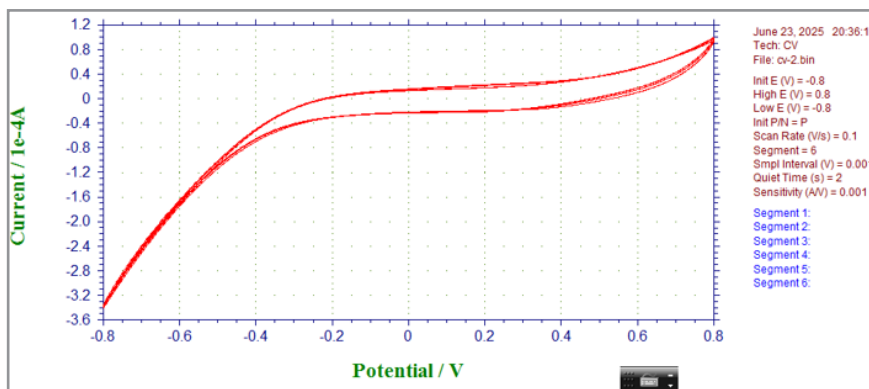


Figure 29: Trial 2

The initial current slightly increases. This indicates enhanced electron transfer kinetics on the surface of the working electrode. There are two potential reasons that can be attributed to this interpretation: a stable formation of biofilm or better contact between microbes and electrodes. Among these two, EAB formation is a more feasible cause to attribute to as its CA trials

displays EAB formation around this time, while soil became relatively dry as time progressed in the unhealthy soil category, which renders the contact between microbes and electrodes poorer (which it makes it unreasonable to confirm the reason being better contact between microbes and electrodes).

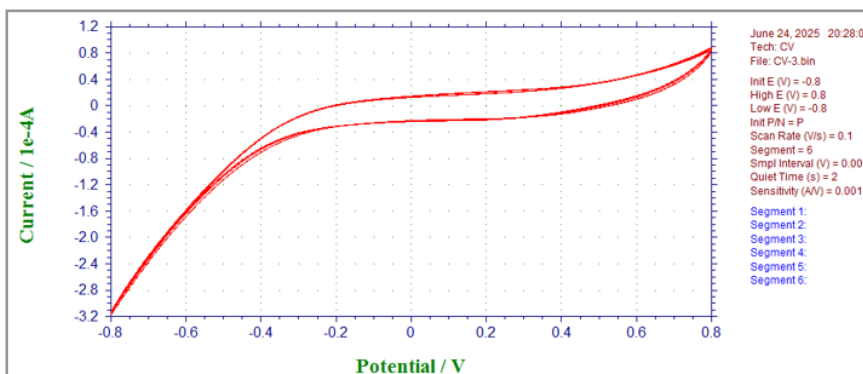


Figure 30: Trial 3

The Initial Current is Maintained. It can be Predicted that EAB is Undergoing Maturation.

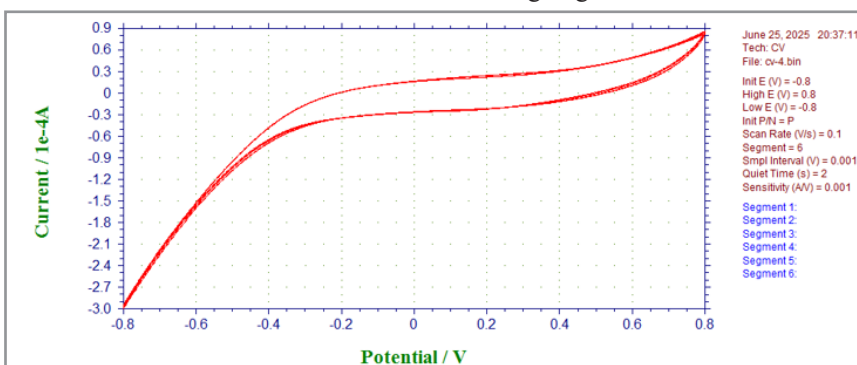


Figure 31: Trial 4

The Initial Current is once Again Slightly Increased.

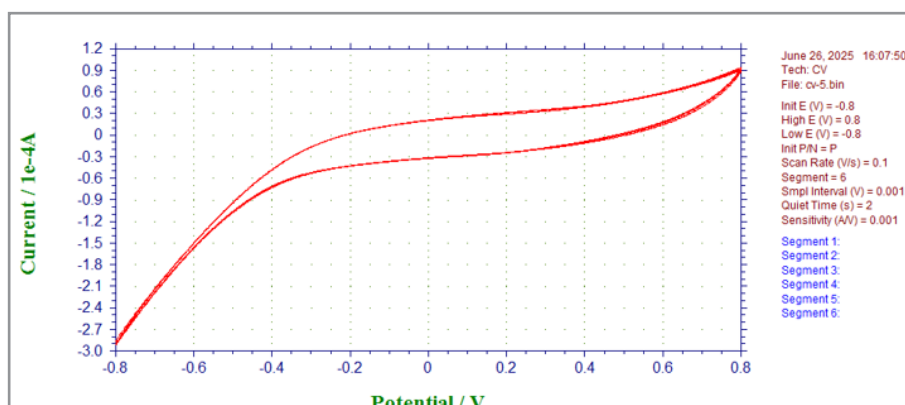


Figure 32: Trial 5

The Initial Current is Maintained.

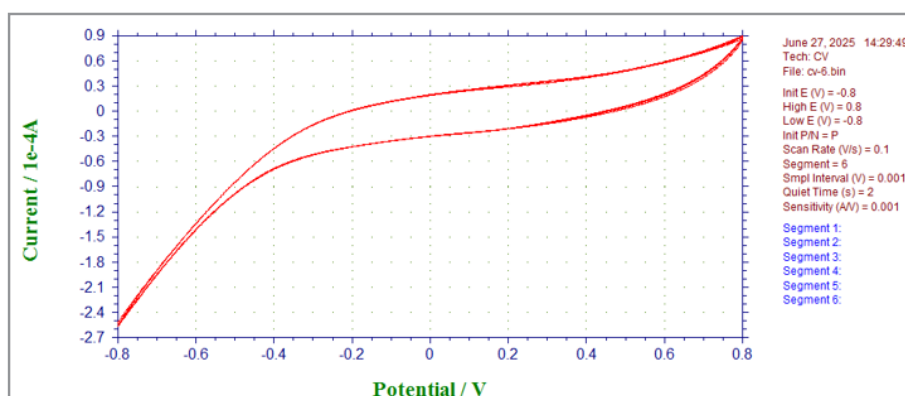


Figure 33: Trial 6

There is a Minor Increase in Initial Current.

CV Data Comparative Overlay

Data plots were overlaid for CV trials in order to visually compare and represent the differences between each trial; these differences will provide various information about soil health and its progress in enhancement including electron transfer, redox activity, biofilm maturation, side reactions, and carbon felt

working electrode stability. Each data plot overlay was created with two consecutive CV graphs - where the old CV trial was overlaid on the one afterwards (the dimensions are based on the more recent version of CV trial) - to analyze exact effects of the BES and EAB formation among it - this facilitates direct comparison and represents the differences in a clearer manner.

Healthy Soil Category

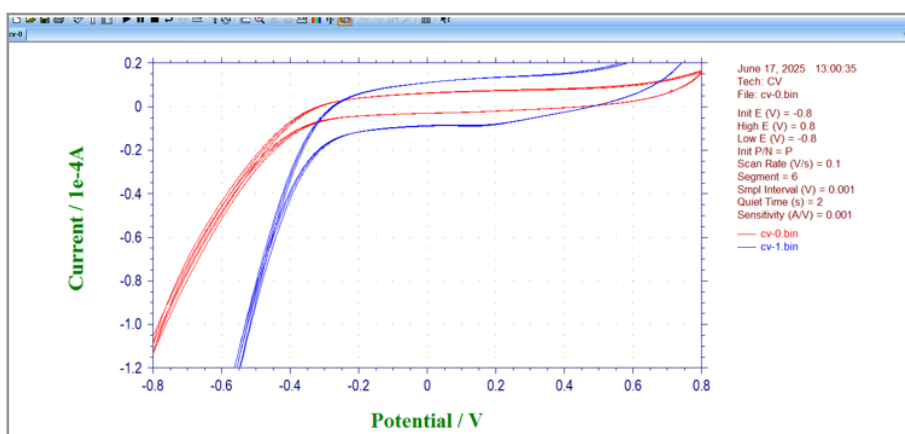


Figure 34: Trial 0 overlaid on Trial 1

This overlay shows that the addition of glucose (both a carbon source and electron donor) into the soil has significantly increased the redox peaks of the graph as displayed in blue line (trial 1). This is because as glucose oxidizes, it releases elec-

trons, which gives rise to increase in current. As a result, this leads to higher redox peak currents and steeper CV slopes. This indicates that the reaction is occurring more rapidly and effectively. The graph displays how addition of glucose itself enabled

a net increase in electron transfer activities as shown from higher cathodic and anodic current.

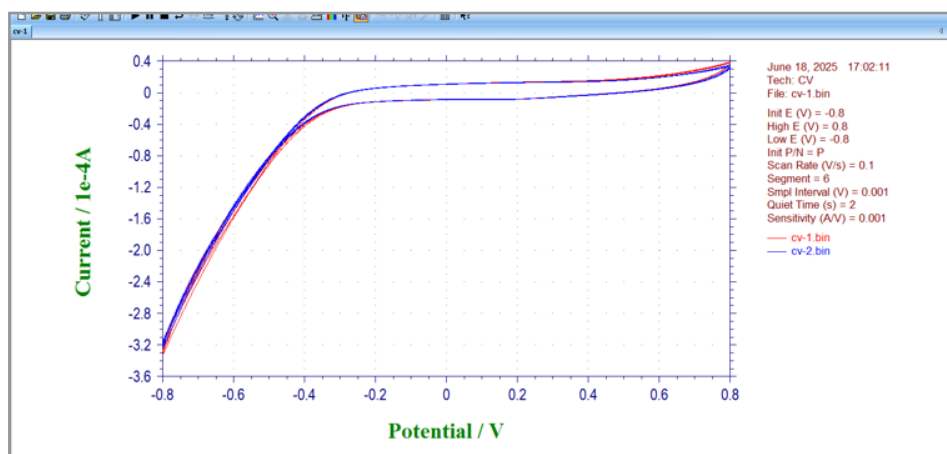


Figure 35: Trial 1 Overlaid on Trial 2

The reason for their high similarity is because they were conducted in a 2 hour time interval, where it is insignificant to expect an occurrence of a considerable change. The graph shape

indicates a moderate redox rise - this suggests that the initial redox processes are forming. In addition, moderate current with rising peak separation indicates early-stage biofilm growth.

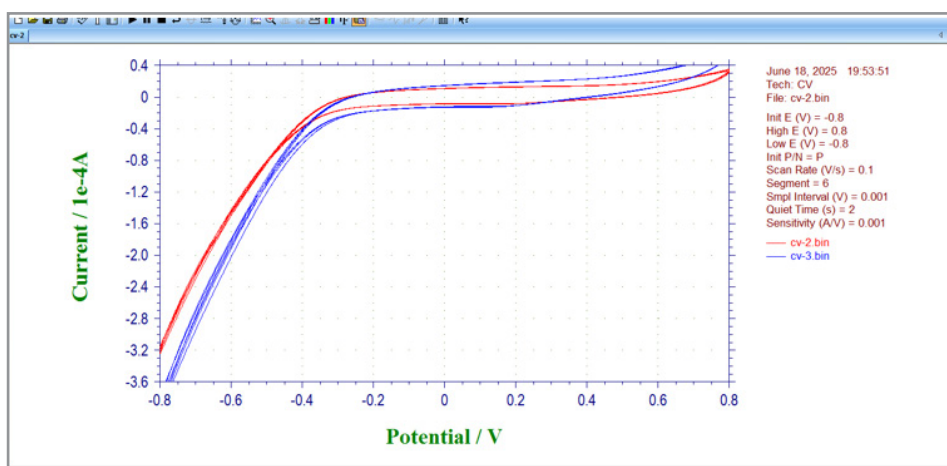


Figure 36: Trial 2 Overlaid on Trial 3

The higher cathodic and anodic current values of trial 3 (blue line) compared to trial 2 indicate a net increase in electron transfer activities compared to trial 2 (red line). The shape of the

graph changes into an increasingly pronounced redox profile - it shows stronger currents and more defined peaks, indicating enhanced microbial extracellular electron transfer.

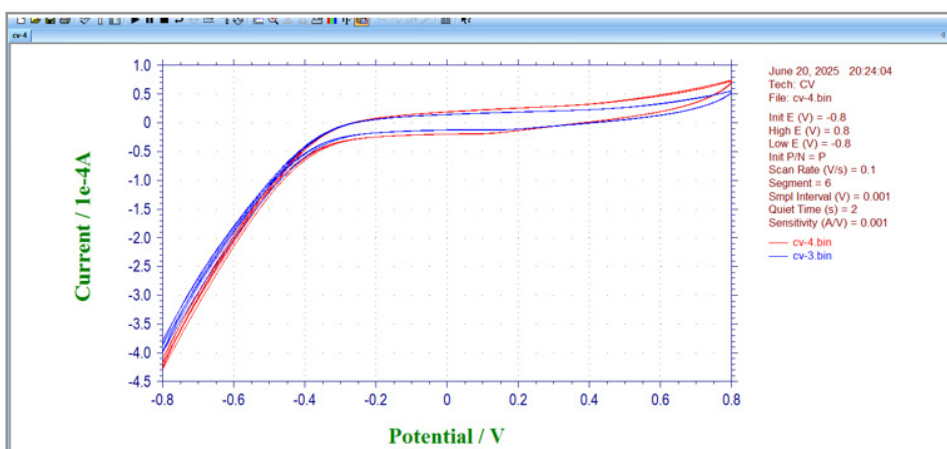


Figure 37: Trial 3 Overlaid on Trial 4

In this CV trial graph overlay, the shape changes in trial 4 to gain distinct peaks and a symmetric loop; the peak clarity and

symmetry indicates healthy, electroactive biofilm. Thus, as EAB is formed, electron transfer kinetics are rapid and controlled.

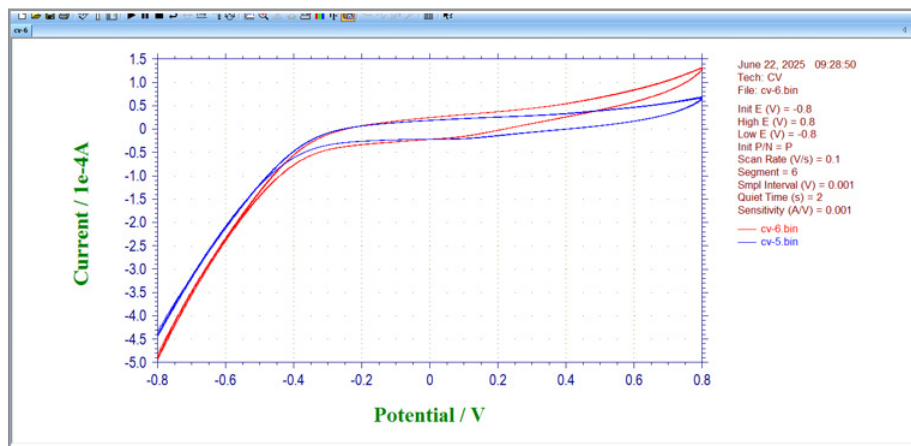


Figure 38: Trial 4 Overlaid on Trial 5

The shape of the graph of trial 5 changes to indicate sharp peaks and have strong responses. As the peak current increases significantly

on trial 5 (red line), it boosts microbial activity and thus engenders effective EET.

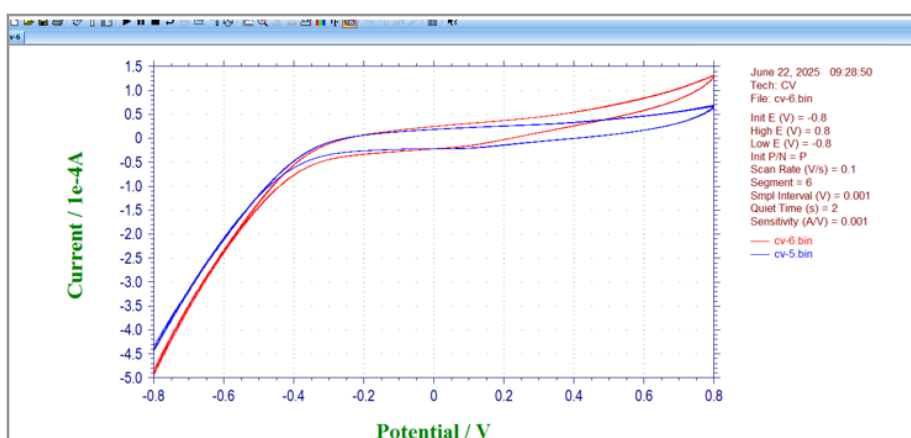


Figure 39: Trial 5 Overlaid on Trial 6

The graph shapes of trial 6 demonstrates the maximum redox peak - showing peak performance of biofilm with efficient and

stable EET. Overall, the electrode-microbe interface is optimal, and the system has acquired a mature and stable EAB layer.

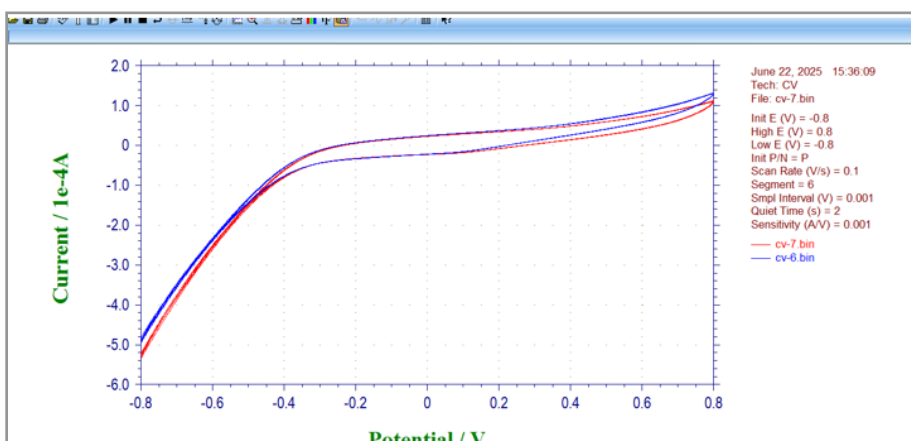


Figure 40: Trial 6 Overlaid on Trial 7

The shape has changed towards broadened strong peaks, and indicates a general mature system. A long term maturity is reached, while incorporating multiple microbial layers; this is because of symmetric cathodic and anodic current peaks as well as minimal variation between these two trials. As the multiple microbial layers are involved, they will allocate roles differently: for instance,

the inner layer directly interfacing with the electrodes to ensure uniform high electroactivity, while the outer layer contributes in structural aspects of the biofilm, in conjunction with how it interacts with nutrients and electrons from soil.

Anodic and cathodic current shift was observed in all of the CV

trial overlays in the healthy soil category. The CV trial overlays actively demonstrated how EAB was effectively formed, and transitioned into long term maturation and stabilization periods; this achieves the objective of this study to sense real-time soil health and initiate EAB formation to remediate soil. This section of CV comparative data overlay also demonstrates that the redox

reactions contributed significantly as it progressed with sharpening of peaks, strong responses, and eventually transitioning into a mature system.

Unhealthy Soil Category

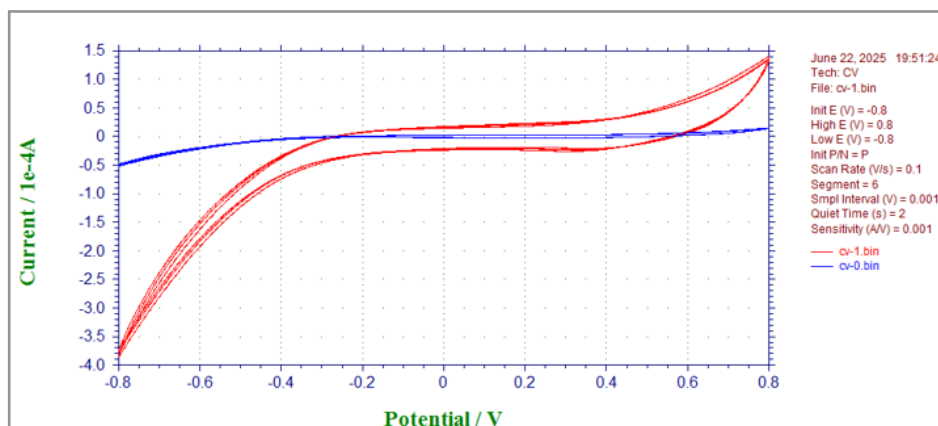


Figure 41: Trial 0 Overlaid on Trial 1

This overlay shows that the addition of glucose (both a carbon source and electron donor of the system) into the soil has significantly increased the redox peaks of the graph as displayed in red line (trial 1). This is because as glucose oxidizes, it releases electrons, which results in an increase in current. As a result, this leads to higher redox peak currents and steeper CV slopes. This indicates that the reaction is occurring in a more rapid and

effective manner. Furthermore, the graph displays how addition of glucose itself enabled a net increase in electron transfer activities in trial 1 as shown from higher cathodic and anodic current values. A notable feature of this graph is that it has the highest anodic and cathodic currents, also having distinct redox peaks which indicate initial bioactivity.

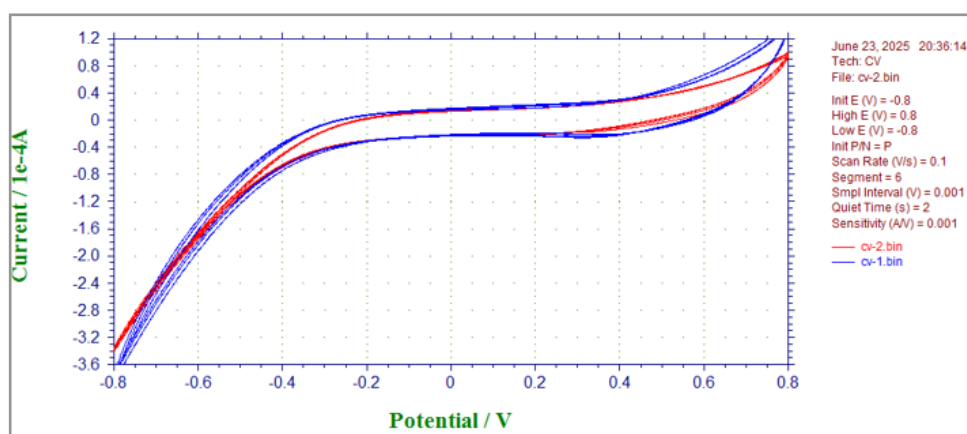


Figure 42: Trial 1 Overlaid on Trial 2

An anodic shift is observed in this graph, showing slight decrease in current from trial 2 to 1, but still indicates redox activ-

ity as the graph has a moderate redox curve.

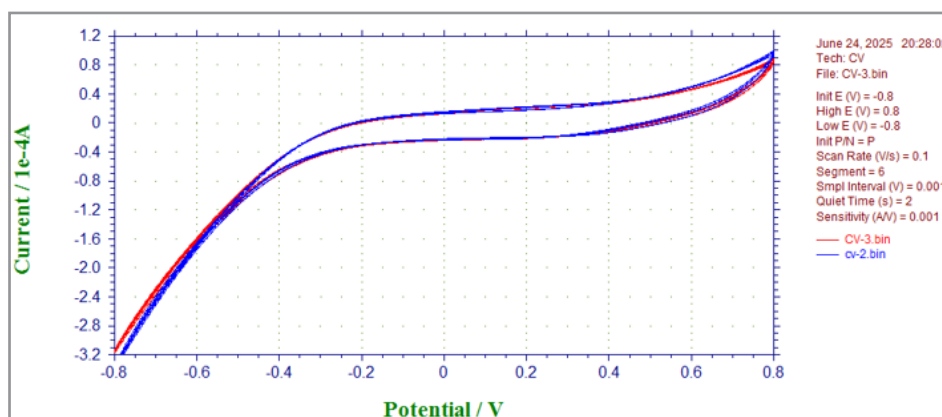


Figure 43: Trial 2 Overlaid on Trial 3

A minimal anodic and cathodic shift is observed in this CV graph overlay. The shape indicates a stable profile along with its

stable current. The slowed electron transfer suggests that EAB is weakly formed and began to mature.

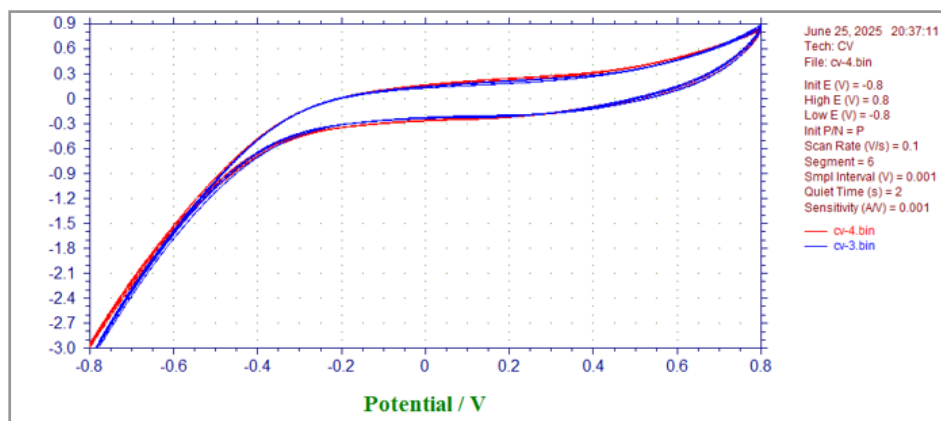


Figure 44: Trial 3 Overlaid on Trial 4

The shape transitions into a capacitive trend from this trial; this suggests that redox activity has faded and double-layer capaci-

tance dominates. Starting from this overlay, there are no more cathodic and anodic shifts observed.

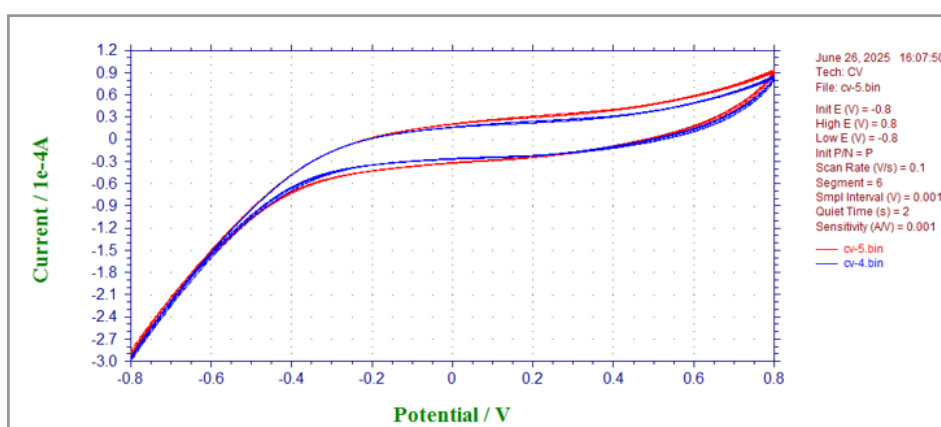


Figure 45: Trial 4 Overlaid on Trial 5

The shape of this graph overlay also shows capacitive trend, persisting its trend from the previous data overlay. This graph shows further weakening of current response as the current range became lower. During the experiment, the texture of the

soil became extremely dry starting from this period. There were no meaningful redox peaks shown from this overlay, which demonstrates weak or inactive electrochemical activity.

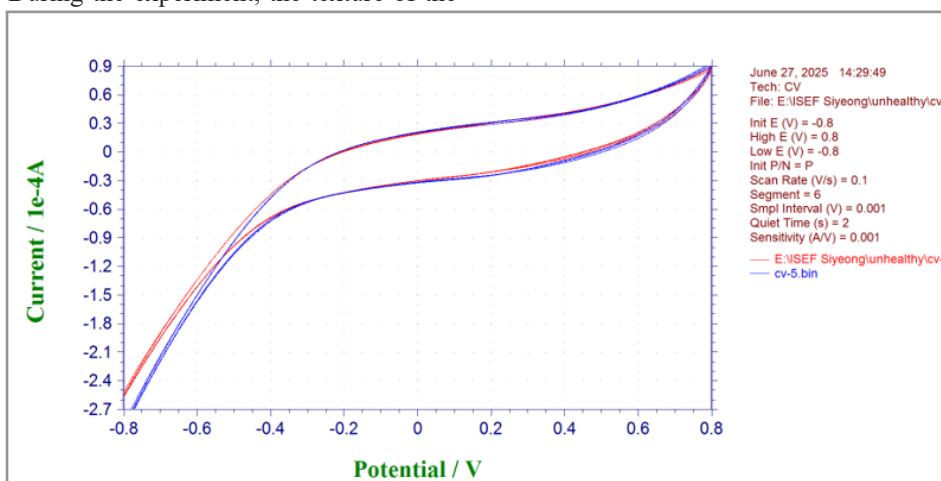


Figure 46: Trial 5 Overlaid on Trial 6

This data overlay has the flattest and weakest curve. Therefore, this graph clearly represents severely unhealthy soil. As a result, it can be implied that the biofilm is dead. This overlay demonstrates a pure capacitive profile.

The CV data comparative overlay was useful in actively comparing each consecutive CV trial on the same dimensions. This enabled a profound level of understanding the results shown through individual CV trials. In the unhealthy soil category, the CV trial overlay actively demonstrates the health conditions of

the soil where the EAB was weak or inactive, which was more difficult to grasp through individual CV trials of the category. Along with other results from this study, the results of the CV overlays directs the future of this research to identify paths to effectively remediate soil after detecting health conditions of it. The future directions and other real-life applications/extensions will be explored more in the discussion of this paper.

pH

The pH data of both healthy and unhealthy soil was collected to directly demonstrate that none of the factors involved in this

BES and the closed loop of the study would impact the pH of the soil. Soil pH is highly influential on soil health as it affects nutrient cycling, fertility, microbial activity and function, and organic matter decomposition [26]. The following data will provide a general overview of how this study of bio electrochemical soil remediation will be feasible in employment in real world applications, ensuring that it does not exacerbate nor provoke soil acidification problems.

Healthy Soil Category

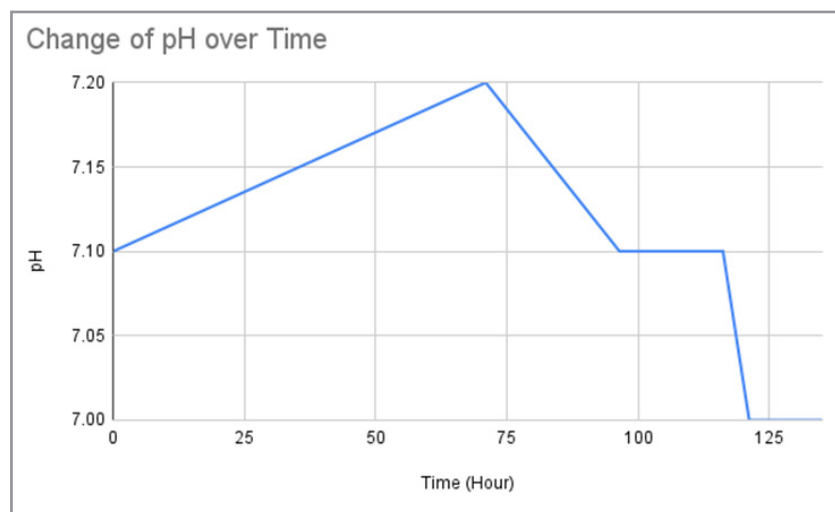


Figure 47: Change of pH over Time

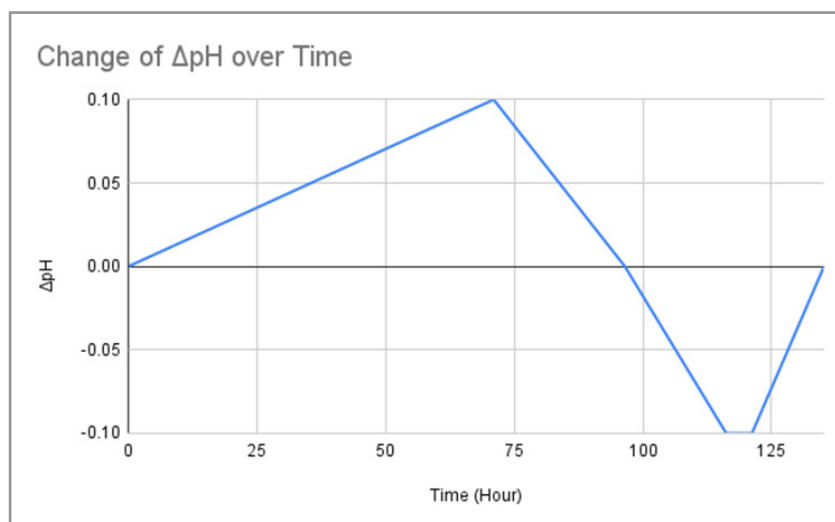


Figure 48: Change of ΔpH over Time:

Assuming that there is ± 0.1 pH parallax error from data interpretation from soil pH meter, these two graphs demonstrate that in the healthy soil category, which have undergone multiple CA and CV trials, show that the pH is stable around pH 7.0 (only fluctuated around ± 0.1 pH on a neutral pH state for approximately 140 hours). Considering that the US Department of Agriculture National Resources Conservation Services specify an optimal pH range for soil to be [6, 7.5], the pH levels indicated from this category align within this range (USDA NRCS, 2022).

In addition, such a minor fluctuation in soil pH further indicates that the methods of this study can be applied in the real world, without exacerbating the soil acidification issues, which brings critical impact for plantation growth and agriculture. While there was a slight decrease in soil pH (acidification), there were also increases (alkalinization) in soil pH, implying a positive outlook of future application of this study.

Unhealthy Soil Category

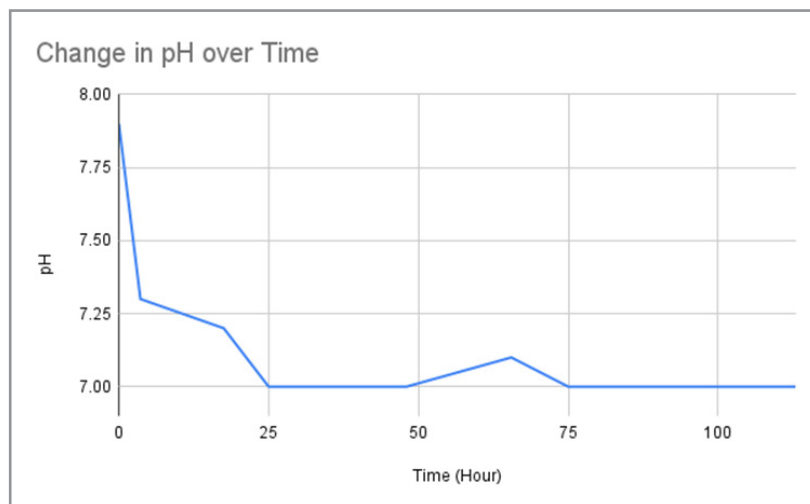


Figure 49: Change of pH over Time:

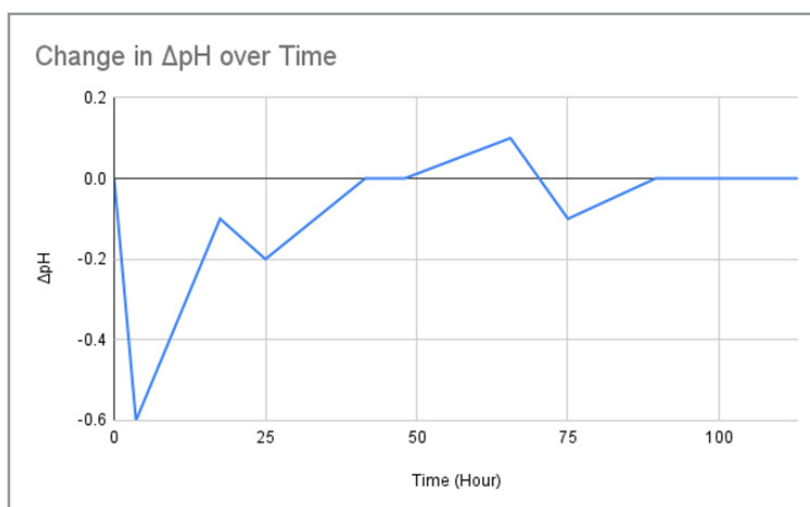
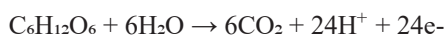


Figure 50: Change of ΔpH over Time

As shown from the ΔpH Vs. Time graph, this shows more frequent fluctuations compared to the healthy soil category. While there were two peaks in the identical graph of healthy soil category, this graph includes 5 different peaks. This shows that the pH variances of the unhealthy soil category were relatively unstable, pH increasing and decreasing quite frequently. The initial soil pH was at 7.9, which is out of the aforementioned optimal soil health range. This shows that unhealthy soil, where micro-organisms were killed through vertical pressure steam sterilizer in intense heat, becomes more alkaline. When pH of the soil was tested after 3.6 hours since the initial measurement, it showed 7.3, and was mostly stabilized around 7.0. This implies that the treatment implemented in this study effectively brought the pH down to the optimal pH range, and enabled stabilization within it. Thus, this further demonstrates how this study has the potential in real world applications as it solves the pH instability of soil.

Redox Peaks, ΔE in CV Trials

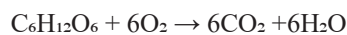
In this particular research, below is the oxidation reaction which takes place at the working electrode:



Below is the reduction reaction which takes place at the counter electrode:



Below is the overall redox coupling - displaying the comprehensive redox reactions within the three-electrode system applied onto the soil environment:



It is important to note that only a single working electrode was employed in this experiment as the three-electrode system was used, thus there are no physical anodes and cathodes involved in this experiment. In the tables below, the anodic/cathodic peak potential/current refers to the maximum and minimum peaks in their respective positions as the redox reactions occurred in the soil during its CV trials. In other words, these terms refer to the redox processes, not the data from the electrodes themselves. Additionally, ΔE refers to the gap between oxidation and reduction peaks. As ΔE increases, this indicates that such a gap widens, signifying higher electron transfer resistance. The anodic peak potential and current are related to the oxidation reactions of this experiment, where the current reflects the reaction itself, while the potential indicates the energy required for the reaction to take place. On the other hand, the cathodic peak potential

and current are related to reduction reactions of this experiment; likewise, the current reflects the reaction itself, while the poten-

tial indicates the energy required for the reaction to occur.

CV Trial (s)	Anodic Peak Potential (V)	Anodic Peak Current (A)	Cathodic Peak Potential (V)	Cathodic Peak Current (A)	ΔE
0	-0.452	1.66E-05	-0.8	-1.13E-04	0.348
1	-0.411	3.89E-05	-0.799	-3.32E-04	0.388
2	-0.411	3.54E-05	-0.799	-3.24E-04	0.388
3	0.799	5.59E-05	-0.8	-4.00E-04	1.599
4	0.799	7.41E-05	-0.799	-4.28E-04	1.598
5	-0.436	6.96E-05	-0.799	-4.43E-04	0.363
6	-0.496	1.32E-04	-0.799	-4.93E-04	0.303
7	-0.463	1.13E-04	-0.799	-5.33E-04	0.336

Figure 51: Healthy Soil CV Redox Peak, ΔE Pairs:

The difference between the stability of anodic and cathodic peak potential is striking in the healthy soil CV trials. While the anodic peak potential keeps on fluctuating and there is an extreme change from -0.411 to 0.799 from 2nd to 4th trial, which then comes back to -0.436 on the fifth trial, the cathodic peak potential maintains a uniform number of -0.8 or -0.799. This indicates

that the energy required for oxidation, which is, for the electron transfer from microbes to electrodes, are in unstable conditions. In comparison, the energy required for reduction - which is the reverse of electron flow direction in oxidation - is relatively stabilized.

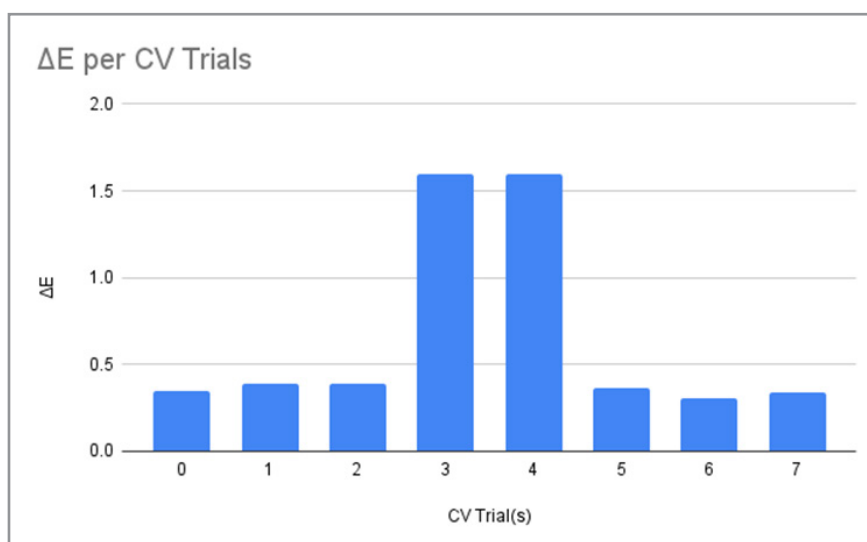


Figure 52: Healthy Soil ΔE per CV Trials

On the third and fourth CV trials - where the testing time was roughly similar to CA trials - there were significant boosts in ΔE ; this aligns with the indication that EAB was formed on electrode surface demonstrated through CA trials 4 and 5. This strongly supports the previous understanding of biofilm formation, and further suggests structural and biochemical changes within the

biofilm, possibly due to the establishment of new redox mediators or developed biofilm architecture. As biofilm thickens, as suggested in comparison between CA trial 5, affecting electron pathways for redox reactions on the EAB, therefore increases ΔE . Overall, these data indicates a significant transition of EAB formation in the soil environment through this experiment.

CV Trial (s)	Anodic Peak Potential (V)	Anodic Peak Current (A)	Cathodic Peak Potential (V)	Cathodic Peak Current (A)	ΔE
0	-0.539	1.53E-05	-0.8	-5.18E-05	0.261
1	-0.572	1.40E-04	-0.8	-3.85E-04	0.228
2	-0.478	9.91E-05	-0.799	-3.41E-04	0.321
3	0.799	8.82E-05	-0.799	-3.17E-04	1.598
4	0.799	8.58E-05	-0.799	-2.99E-04	1.598
5	-0.467	9.40E-05	-0.799	-2.91E-04	0.332
6	-0.51	8.96E-05	-0.798	-2.56E-04	0.288

Figure 53: Unhealthy Soil CV Anodic Peak and Cathodic Peak Pair

There are multiple similarities that could be identified between healthy and unhealthy soil categories of anodic and cathodic peaks. To begin with, there were both significant boosts in the amount of ΔE in trial 3 and 4, which is attributed to the factor of EAB formation on the working electrode surface. Additionally, the values of ΔE in other trials - meaning trials before and after trial 3 and 4 - are similar. These similarities both imply that both soil categories underwent EAB formation and maturation period. Final similarity to note is the cathodic peak potential of both categories where they are at the extreme end of the potential settings in the CV trials (the minimum potential set as the parameter was -0.8 V). As previously stated this indicates that the

energy required for oxidation, which is, for the electron transfer from microbes to electrodes, are unstable. Some recognizable difference from unhealthy soil category is that its anodic peak current is mostly low with minimal change and negative trend while healthy soil category steadily increases its anodic peak current. A decrease in anodic peak current directly correlates to the decrease of the oxidation current, which is caused by loss of electroactive microbial activity, engendering the EAB to become inactive - this idea aligns adequately with the findings from the analysis of CV data comparative overlay, especially the overlay of trial 4 onto 5 and trial 5 onto 6.

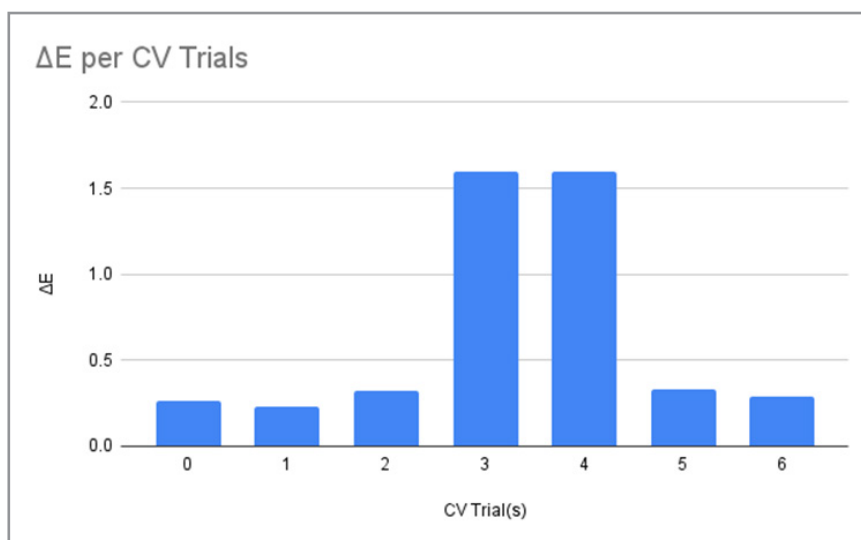


Figure 54: Unhealthy Soil ΔE per CV Trials

Same as the healthy soil category, the ΔE of CV trials 3 and 4 is striking. Although they indicate EAB formation similar to the interpretation made on the healthy soil category, this EAB is not mature and not stable enough to remediate soil, suggested from previous CA and CV trials. In contrast with how the biofilm thickened, redox reactions were enhanced, and electron transfer was improved, the EAB from this category was not capable of providing such merits - which can be attributed to lack of active microorganisms to form microbial communities, then forming EAB.

Discussion

In conclusion, the results show that the CA and CV trials effectively reflect the health conditions of both healthy and unhealthy soil categories. In addition, the results show that both healthy and unhealthy soil categories formed EAB; nevertheless, they had different implications. Specifically, while the healthy soil category formed sturdy EAB structure as a result from its richness in microorganism content, unhealthy soil category formed a relatively weak EAB structure due to lack or absence of microorganism content as it was killed by putting the healthy soil into the vertical pressure steam sterilizer. Furthermore, this process did not exacerbate soil acidification problems, while there were instances where excessively high pH was dropped into the optimal soil pH range (set by USDA NRCS). Overall, this study has succeeded in the aspect of real-time electrochemical assessment of soil health.

Considering that approximately 33% of world's soil is moder-

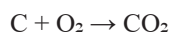
ately to highly degraded, while it is projected that 95% of global soil would be degraded by 2025, the next step ahead of this research is to not only assess the health conditions of soil in a bio electrochemical approach but also remediating soil accordingly after a deep level of real time analysis [27, 28]. Currently, this research has shown potential through stabilizing the pH of the unhealthy soil category, but the CA and CV trials of unhealthy soil category suggests that a weak EAB was formed, not providing the advantages as indicated from the healthy soil category. Another next step to consider taking is employing this method to enhance carbon sequestration. In the status quo, the idea proposed from this study is capable of carbon sequestration to a certain extent as it enhances electroactive microbial activity, decomposing organic materials to carbon and fixing it via microbial metabolism. As a method for enhancement of electroactive microbial activity is figured out, this will enhance soil's carbon sequestration capacity to a broader range of soil types.

This study incorporates positive impacts on soil's carbon sequestration capacities, contributing towards climate change mitigation. To begin with, electrochemical soil remediation and microbial stimulation helps restore soil aggregation, which protects organic matter from enzymatic degradation. Consequently, protected carbon, which is, carbon inside aggregates, are less accessible to decomposers, aiding long-term carbon storage in soil. Additionally, EABs are made of EPS. EPS refers to a matrix of high molecular weight substances, which is composed of polysaccharides, proteins, and nucleic acids that are secreted by microbes. EPS production from this system leads to effective

carbon storage as its secretion by microbes fixes organic carbon into stable macromolecules in the soil environment. Then, EPS physically protects microbial cells, functioning like a glue to bind soil particles into aggregates. Furthermore, the complex structure of EPS molecules resists microbial breakdown, ensuring that sequestered carbon resides in the soil for an increased period of time. Overall, EPS production protects sequestered carbon physically in biofilms and aggregates, chemically stabilizes sequestered carbon for centuries through bonding with other minerals to create organ mineral complexes, and retains biologically by preventing microbial breakdown. Although carbon sequestration cannot be directly quantified through utilizing previous bio electrochemical techniques, it is possible to infer it through observing the displayed trends of microbial growth, EPS accumulation, and biofilm maturation actively demonstrated from CA and CV trials. To illustrate, CA trials such as trial 6 and 7 from healthy soil category suggests EAB maturation and optimization, demonstrating that carbon sequestration abilities are enhanced. Additionally, CV trials such as trial 3 and 4, where anodic and cathodic peak potential broadens and double layer capacitance increases, those factors thereby increase fixed storing of carbon. Soil is the second largest carbon sink globally, and restoring its health in a proper way will enable optimal exploitation of soil's carbon sequestration abilities.

In fact, 3.67 tons of carbon dioxide in earth's atmosphere converts to only 1 ton of carbon stored in soil (through photosynthesis of plantation). This is because carbon dioxide, which is in a gas state when in the atmosphere, gets transformed into organic matter of carbon - which is commonly referred to as soil organic carbon. This can also be represented through a chemical reaction of pure carbon combustion (a chemical reaction between a fuel and oxygen that produces heat, light, and new chemical products like CO₂ and H₂O).

Below is the Chemical Reaction



The atomic mass of carbon = 12

molecular mass of oxygen = 16*2 = 32

molecular mass of carbon dioxide = 12+32 = 44

Therefore, the Ratio is:

Mass of CO₂ / Mass of C = 44/12 \approx 3.67 (rounded 2 decimal points)

As a result, a ton of carbon absorbed from a plant means 3.67 tons of carbon dioxide removed from the atmosphere.

As these two other aspects are considered and developed (active soil remediation and carbon sequestration), this solution will be able to not only detect health conditions of soil but also actively rejuvenate and restore soil health, enabling it to perform in its maximum capacity to contribute in climate change mitigation.

Engineering Extension

The following engineering extension can be executed in order to leverage the findings from this study as well as addressing its key limitation of failure to form robust EAB in unhealthy soil category. Through multiple data sets and its analysis acquired through this study, insufficiency of microbial community structure was attributed to the flawed formation of EAB. To extend the findings from this study to extend from diagnosing soil health

towards actively remediating soil based on their analyzed health conditions, the following engineering extension is proposed on a theoretical basis.

Recognizing the lack of sufficient microbial activity to form EABs especially from the unhealthy soil category, this system automates microbial stimulation and nutrient release to surpass the level of solely assessing health, but also actively remediating the soil. The workflow of this product is to initially diagnose soil health, where the three-electrode system performs CV and CA trials to assess microbial health of soil, which was already successfully done within this study. Then, the AI decision making system built based on all of the CA and CV trial results from this research will provide an evaluation of current status of soil conditions and recommend next actions to consider along with specifying each recommendations' confidence, rationale, technical details, and expected outcomes (which are based on the data collected from previous experiments as well as its simulation). The AI model reaches the analysis through comparing the data from the physical experiment outcomes and its simulation. For instance, when the signal falls behind the threshold due to poor electrochemical activity, it recommends remediation, and when the microbial community is sturdy enough, it recommends limiting external intervention. In particular to actively remediating soil, which is the primary purpose of this engineering extension, it will utilize a mechanism of pressurized microbial cartridges with electrothermal release, where microbial consortia are released into the rhizosphere as wax membrane is heated up by applying a short electric pulse. In addition to this, alginate beads serve as a secondary reinforcement to microencapsulate microbes in calcium alginate (secondary microbe batch) activated based on pH levels (specifically, when pH is below 6.5 or above 7.6, when it is out of the optimal soil range), then coat with biodegradable materials to ensure minimal impact in the soil environment. Specifically, the biodegradable materials being softwood sawdust as a coating material over a mycelium-cork composite. Simultaneously, electrochemical stimulation is applied through CV and CA trials, initiating redox cycling, thus enhancing EET and microbial metabolism. Meanwhile, the outer cellulose biodegradable mesh that microencapsulated microbes progressively breaks down, releasing crucial nutrients to remediate soil safely.

One common concern that could emerge regarding this active remediation sequence is the feasibility of effective dispersion of the microbial consortia and micronutrients. In order to address this concern, the system of this extension will exploit electrokinetic migration. Electrokinetic migration refers to movement of charged particles or ions, which are primarily microbes in this particular experiment, toward an electrode of opposite charge due to an electric field. In the three-electrode system the charges will flow between the working and counter electrode but not at the reference electrode as it was not designed to pass current. Considering that bacteria's cell membranes, which are composed of lipopolysaccharides and teichoic acids, have a net negative surface charge, they will migrate towards the positive charge. In the three electrode systems of this study, the working electrode constantly applies current to the soil from its CA trials, rendering it positive; in contrast, the counter electrode has a negative charge. Therefore, bacteria will be migrating towards working electrodes, effectively spreading micronutrients and forming EAB across the soil.

The advantage of employment of electro kinetic migration is that its transportation can fundamentally take place over distances in both compact or poorly permeable soils. The migration typically works when a weak DC electric field is applied. However, considering that CA trials itself already applies constant current

to soil, there is no need to add additional electrode systems; instead, it solely requires a slight modification of applied current of 0.2V (original parameters set for previous CA trials) to 1V.

System Components

The following is the Overview of System Components of the Engineering Extension:

Component	Specifics	Function
Three-Electrode System (Same system as the experiment, consists of working, counter, and reference electrode)		Employed for CV and CA trials, EAB formation, and active redox cycling
	Active Electrochemical Redox Cycling	Controlled polarity pulses stimulate microbial metabolism and pollutant breakdown
Inoculation System	Electrothermal Wax-Catridge	Triggered as wax membrane is heated, releasing microbial consortia into the soil
	Alginate Beads Enclosed with Biodegradable Outer Mesh	pH-activated release of secondary microbes into the soil, enclosed with cellulose based outer mesh that degrades about 2-4 weeks
Microcontroller Managed Circuit		A microcontroller to supervise the overall CV and CA trial runs, integrated with website and AI for analysis and decision making, and remediation through controlling inoculation systems

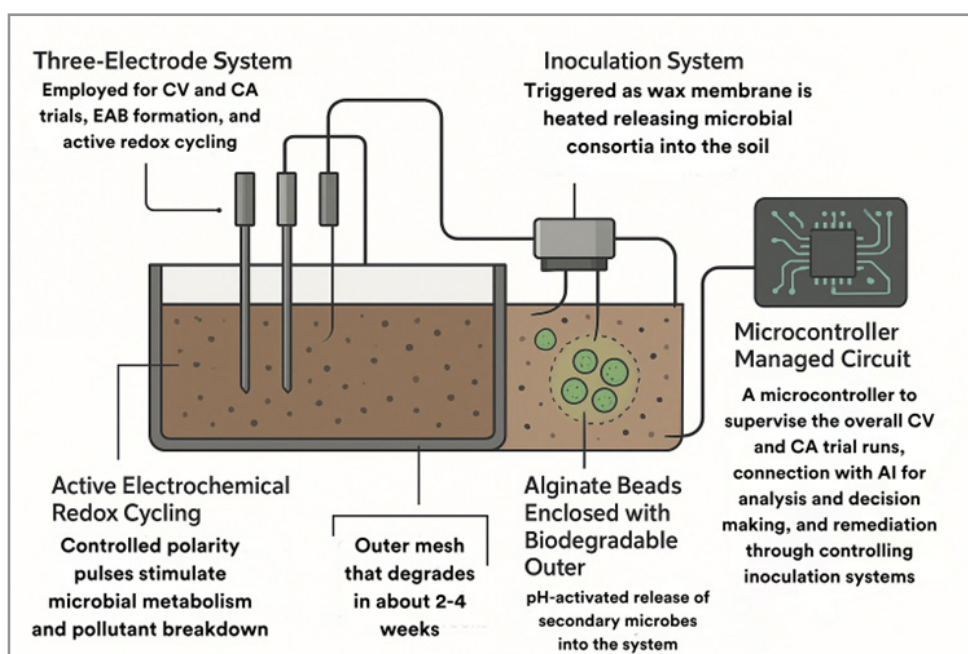


Figure 55: AI Generated image of the Overall System

Sample Website and AI Integration

The following website (URL: <https://isefprojectbyjohn.netlify.app/>) is a sample website for presenting this engineering extension, where the users can experience the simulation of what the engineering extension would do in real life.

The website itself has multiple key features. To begin with, it runs sample CA and CV trials in dual modes - sensing and remediation. During the sensing mode, there are no microbes or any type of supplement released to the system. It is used for

analyzing the impact of soil remediation efforts done within the website or comparing between before and after a certain action was performed within the system. During the remediation mode, it actively releases microbes through the system's electrothermal wax cartridge and alginate beads enclosed with biodegradable outer mesh, based on the conditions of the soil. Redox cycling can also be employed for remediation, to effectively form strong EABs. Meanwhile, CA and CV trials alternate, where each trial is performed based on the needs of the user. To illustrate, if the user needs to detect and confirm EAB formation, or observe the

redox activity of the system, they could observe CA trials; whereas, if the users are looking for tracking changes and comparing bio electrochemical activity, they could observe CV trials. Users can activate AI decision mode in order to receive recommendations on the soil health indicated from CA and CV simulation trials. The lines of the graphs are color coded in order to differentiate between results during sensing and remediation modes. Additionally, users can upload their own CA and CV trials, which will be analyzed by the AI based on the CA and CV results of this study, to provide detailed analysis and recommendation for future action to effectively remediate soil. Furthermore, AI can also make decisions based on the analysis on the sample CA and CV trials run on the website. It then provides recommendations along with a rationale, expected outcomes, and the confidence of its recommendation. Finally, there is a system event log, where users can easily view the actions that they have taken within this sample soil system, or within their uploaded CV or CA data set.

Implications and Challenges

The proposed engineering extension effectively integrates the efficient real-time electrochemical biosensing validated through this research with potential methods of real-time soil remediation based on such electrochemical biosensing. This new approach brings value to the realms of the research as it enables in-situ, nondestructive methods of soil biosensing as well as soil remediation. By implementing soil remediation, it enhances the soil's carbon sequestration abilities, contributing to climate change mitigation. By implementing effective formation of EPS and EAB, this can render soil to become a more effective carbon sink. In addition, this research opened potential for integration between soil data and AI, which can help train AI models to provide more accurate predictions and more effective decisions to remediate soil effectively. Finally, this engineering extension can be potentially employed in the field of sustainable agriculture, where individuals can easily gain a better understanding about soil health, helping them with crop rotation, fertilizer usage, and land regeneration efforts strategies. All in all, this extension effectively connects diagnosis and suggestion of action plans based on it.

Despite the diverse advantages of this engineering extension, there are remaining limitations and challenges that should be considered for future studies and reference. To begin with, the accuracy of the prediction of the AI model might be unstable and weak considering applications in wild soil settings. This is because the data gathered through this experiment were lab based, thus it cannot fully consider every aspect of the soil environment. One key factor that was not considered in this research was weather/climate, as it was enclosed in a parafilm limiting influence from temperature and humidity. Also, it was not tested in a rainy environment, which could influence soil texture, structure, noise influence, and pH. It is undeniable that the ecosystem is non-linear and context-dependent; unexpected changes may give rise to significant implications, which were not fully explored in this research. In addition, the unpredictability of cells' redirection of resources is a challenge to note of this engineering extension. There are various reasons for this behaviour, one being non-genetic heterogeneity; which determines cell fate decision and differential response and adaptation to different environmental conditions [29]. Another reason is due to bet-hedg

Sample Website and AI Integration

The following website (URL: <https://isefprojectbyjohn.netlify.app/>) is a sample website for presenting this engineering extension, where the users can experience the simulation of what the engineering extension would do in real life.

The website itself has multiple key features. To begin with, it runs sample CA and CV trials in dual modes - sensing and remediation. During the sensing mode, there are no microbes or any type of supplement released to the system. It is used for analyzing the impact of soil remediation efforts done within the website or comparing between before and after a certain action was performed within the system. During the remediation mode, it actively releases microbes through the system's electrothermal wax cartridge and alginate beads enclosed with biodegradable outer mesh, based on the conditions of the soil. Redox cycling can also be employed for remediation, to effectively form strong EABs. Meanwhile, CA and CV trials alternate, where each trial is performed based on the needs of the user. To illustrate, if the user needs to detect and confirm EAB formation, or observe the redox activity of the system, they could observe CA trials; whereas, if the users are looking for tracking changes and comparing bio electrochemical activity, they could observe CV trials. Users can activate AI decision mode in order to receive recommendations on the soil health indicated from CA and CV simulation trials. The lines of the graphs are color coded in order to differentiate between results during sensing and remediation modes. Additionally, users can upload their own CA and CV trials, which will be analyzed by the AI based on the CA and CV results of this study, to provide detailed analysis and recommendation for future action to effectively remediate soil. Furthermore, AI can also make decisions based on the analysis on the sample CA and CV trials run on the website. It then provides recommendations along with a rationale, expected outcomes, and the confidence of its recommendation. Finally, there is a system event log, where users can easily view the actions that they have taken within this sample soil system, or within their uploaded CV or CA data set.

Implications and Challenges

The proposed engineering extension effectively integrates the efficient real-time electrochemical biosensing validated through this research with potential methods of real-time soil remediation based on such electrochemical biosensing. This new approach brings value to the realms of the research as it enables in-situ, nondestructive methods of soil biosensing as well as soil remediation. By implementing soil remediation, it enhances the soil's carbon sequestration abilities, contributing to climate change mitigation. By implementing effective formation of EPS and EAB, this can render soil to become a more effective carbon sink. In addition, this research opened potential for integration between soil data and AI, which can help train AI models to provide more accurate predictions and more effective decisions to remediate soil effectively. Finally, this engineering extension can be potentially employed in the field of sustainable agriculture, where individuals can easily gain a better understanding about soil health, helping them with crop rotation, fertilizer usage, and land regeneration efforts strategies. All in all, this extension effectively connects diagnosis and suggestion of action plans based on it.

Despite the diverse advantages of this engineering extension,

there are remaining limitations and challenges that should be considered for future studies and reference. To begin with, the accuracy of the prediction of the AI model might be unstable and weak considering applications in wild soil settings. This is because the data gathered through this experiment were lab based, thus it cannot fully consider every aspect of the soil environment. One key factor that was not considered in this research was weather/climate, as it was enclosed in a parafilm limiting influence from temperature and humidity. Also, it was not tested in a rainy environment, which could influence soil texture, structure, noise influence, and pH. It is undeniable that the ecosystem is non-linear and context-dependent; unexpected changes may give rise to significant implications, which were not fully explored in this research. In addition, the unpredictability of cells' redirection of resources is a challenge to note of this engineering extension. There are various reasons for this behaviour, one being non-genetic heterogeneity; which determines cell fate decision and differential response and adaptation to different environmental conditions [29]. Another reason is due to bet-hedging, an intentional risk spreading strategy to improve survival. In particular, bacteria produce persister cells by reallocating metabolic resources, which is a classic bet hedging strategy to survive antibiotic stress [30]. Generally, by having subpopulation of the soil be in diverse conditions, for instance, slowed down growth or dormancy, it helps the soil to survive unpredictable future stress; this is the rationale of bet-hedging [31]. As cells redirect resources in unpredictable manner, this gives rise to yield drops and hinders effective use of microbial consortia additions. Overall, this behaviour of cells lowers the efficiency of the system. Generally, these limitations and challenges are tied with the unpredictable nature of soil due to its behaviour in pursuit of survival and efficiency; it is highly encouraged for future studies to consider this factor and adequately address them to make soil health evaluation and soil remediation more feasible via electrochemistry in real world applications [32-36].

Acknowledgements

I would like to express sincere gratitude for Professor 朴云仙 for her guidance, feedback, and invitation to Jilin University to conduct this study, and her PhD students in providing technical support at the lab. It was an honor to be invited to conduct this research at Jilin University.

References

- Levis, S. (2010). Modeling vegetation and land use in models of the Earth System. *Wiley Interdisciplinary Reviews: Climate Change*, 1(6), 840–856. <https://doi.org/10.1002/wcc.83>
- Pütz, S., Groeneveld, J., Henle, K., Knogge, C., Martensen, A. C., Metz, M., Metzger, J. P., Ribeiro, M. C., de Paula, M. D., & Huth, A. (2014). Long-term carbon loss in fragmented Neotropical forests. *Nature Communications*, 5(1). <https://doi.org/10.1038/ncomms6037>
- Dynarski, K. A., Bossio, D. A., & Scow, K. M. (2020). Dynamic stability of soil carbon: Reassessing the “permanence” of soil carbon sequestration. *Frontiers in Environmental Science*, 8. <https://doi.org/10.3389/fenvs.2020.514701>
- Noronha, R. F., Snepken, K., & Kaneko, K. (2025). Modelling soil as a living system: Feedback between microbial activity and spatial structure. *ArXiv.org*. <https://arxiv.org/abs/2502.20662>
- Buckeridge, K. M., Creamer, C., & Whitaker, J. (2022). Deconstructing the microbial necromass continuum to inform soil carbon sequestration. *Functional Ecology*, 36(6), 1396–1410. <https://doi.org/10.1111/1365-2435.14014>
- Dunne, D. (2017, August 25). World's soils have lost 133bn tonnes of carbon since the dawn of agriculture. *Carbon Brief*. <https://www.carbonbrief.org/worlds-soils-have-lost-133bn-tonnes-of-carbon-since-the-dawn-of-agriculture/>
- Food and Agriculture Organization of the United Nations. (2021, November 6). COP26: Agricultural expansion drives almost 90 percent of global deforestation. *FAO*. <https://www.fao.org/newsroom/detail/cop26-agricultural-expansion-drives-almost-90-percent-of-global-deforestation/en>
- Dhakane, A. A., Osman, F. M., Afrah, N. A., & Ahmed, A. O. (2024). The effect of deforestation on agriculture production. *IOSR Journal of Agriculture and Veterinary Science*, 17(06), 45–49. <https://doi.org/10.9790/2380-1706014549>
- Wingender, J., Neu, T. R., & Flemming, H.-C. (1999). What are bacterial extracellular polymeric substances? In *Microbial Extracellular Polymeric Substances* (pp. 1–19). https://doi.org/10.1007/978-3-642-60147-7_1
- ScienceDirect Topics. (n.d.). Biofilms – an overview. *ScienceDirect*. <https://www.sciencedirect.com/topics/materials-science/biofilms>
- Kilic, T., & Bali, E. B. (2023). Biofilm control strategies in the light of biofilm-forming microorganisms. *World Journal of Microbiology & Biotechnology*, 39(5). <https://doi.org/10.1007/s11274-023-03584-6>
- Siddharth, T., Sridhar, P., Vinila, V., & Tyagi, R. D. (2021). Environmental applications of microbial extracellular polymeric substance (EPS): A review. *Journal of Environmental Management*, 287, 112307. <https://doi.org/10.1016/j.jenvman.2021.112307>
- Kayoumu, M., Wang, H., & Duan, G. (2025). Interactions between microbial extracellular polymeric substances and biochar, and their potential applications: A review. *Biochar*, 7(1). <https://doi.org/10.1007/s42773-025-00452-4>
- Zhuo, M., Quan, X., Yin, R., & Lv, K. (2024). Enhancing methane production and interspecies electron transfer of anaerobic granular sludge by the immobilization of magnetic biochar. *Chemosphere*, 352, 141332. <https://doi.org/10.1016/j.chemosphere.2024.141332>
- Engel, C., Schattenberg, F., Dohnt, K., Schröder, U., Müller, S., & Krull, R. (2019). Long-term behavior of defined mixed cultures of *Geobacter sulfurreducens* and *Shewanella oneidensis* in bioelectrochemical systems. *Frontiers in Bioengineering and Biotechnology*, 7. <https://doi.org/10.3389/fbioe.2019.00060>
- BOQU. (2024, May 15). Analyzing redox status in soil and compost for optimal plant growth. *Boquinstrument.com*. <https://www.boquinstrument.com/a-news-analyzing-redox-status-in-soil-and-compost-for-optimal-plant-growth.html>
- Mohamed, A., Sanchez, E., Sanchez, N., Friesen, M. L., & Beyenal, H. (2021). Electrochemically active biofilms as an indicator of soil health. *Journal of the Electrochemical Society*, 168(8), 087511. <https://doi.org/10.1149/1945-7111/ac1e56>
- Qi, B., Zhang, K., Qin, S., Lyu, D., & He, J. (2022). Glucose addition promotes C fixation and bacteria diversity in C-poor soils, improves root morphology, and enhances key N metabolism in apple roots. *PLOS ONE*, 17(1), e0262691.

<https://doi.org/10.1371/journal.pone.0262691>

19. Zhou, W., Qin, X., Lyu, D., & Qin, S. (2021). Effect of glucose on the soil bacterial diversity and function in the rhizosphere of *Cerasus sachalinensis*. *Horticultural Plant Journal*, 7(4), 307–317. <https://doi.org/10.1016/j.hpj.2021.02.002>
20. Babauta, J., Renslow, R., Lewandowski, Z., & Beyenal, H. (2012). Electrochemically active biofilms: Facts and fiction. A review. *Biofouling*, 28(8), 789–812. <https://doi.org/10.1080/08927014.2012.710324>
21. Li, F., Yu, H., Zhang, B., Hu, C., Lan, F., Wang, Y., You, Z., Liu, Q., Tang, R., Zhang, J., Li, C., Shi, L., Li, W., Neelson, K. H., Liu, Z., & Song, H. (2024). Engineered cell elongation promotes extracellular electron transfer of *Shewanella oneidensis*. *Advanced Science*. <https://doi.org/10.1002/advs.202403067>
22. Rimboud, M., Bergel, A., & Erable, B. (2016). Multiple electron transfer systems in oxygen reducing biocathodes revealed by different conditions of aeration/agitation. *Bioelectrochemistry*, 110, 46–51. <https://doi.org/10.1016/j.bioelechem.2016.03.002>
23. Pine Research Instrumentation. (2018). Cyclic voltammetry (CV). [pineresearch.com](https://pineresearch.com/support-article/cyclic-voltammetry-cv/). <https://pineresearch.com/support-article/cyclic-voltammetry-cv/>
24. Goebes, P., Schmidt, K., Seitz, S., Both, S., Bruelheide, H., Erfmeier, A., Scholten, T., & Kühn, P. (2019). The strength of soil–plant interactions under forest is related to a critical soil depth. *Scientific Reports*, 9(1). <https://doi.org/10.1038/s41598-019-45156-5>
25. Raj, S., Ganamuthu, H. L., Ashokkumar, V., Govindarajan, G., Kandasamy, S., & Zhang, H. (2020). Biofilm formation and electrochemical metabolic activity of *Ochrobactrum* sp. JSRB-1 and *Cupriavidus* sp. JSRB-2 for energy production. *Environmental Technology & Innovation*, 20, 101145. <https://doi.org/10.1016/j.eti.2020.101145>
26. Mosley, L. M., Rengasamy, P., & Fitzpatrick, R. (2024). Soil pH: Techniques, challenges and insights from a global dataset. *European Journal of Soil Science*, 75(6). <https://doi.org/10.1111/ejss.70021>
27. United Nations Office for Disaster Risk Reduction. (2023, June 7). Soil degradation. UNDRR. <https://www.undrr.org/understanding-disaster-risk/terminology/hips/en0005>
28. Earth.org. (2024, June 17). 95% of the Earth's land set to be degraded by 2050. Save Soil. <https://earth.org/95-of-the-earths-soil-on-course-to-be-degraded-by-2050/>
29. Capp, J.-P., Jolly, M. K., & Sharma, A. (2021). Editorial: Non-genetic heterogeneity in development and disease. *Frontiers in Genetics*, 12. <https://doi.org/10.3389/fgene.2021.731814>
30. Morales, D., Micheva-Viteva, S., Adikari, S., Werner, J., Wolinsky, M., Hong-Geller, E., Kim, J., & Ojima, I. (2022). Targeting the bet-hedging strategy with an inhibitor of bacterial efflux capacity enhances antibiotic efficiency and ameliorates bacterial persistence in vitro. *Microorganisms*, 10(10), 1966. <https://doi.org/10.3390/microorganisms10101966>
31. ScienceDirect Topics. (n.d.). Bet-hedging – an overview. ScienceDirect. <https://www.sciencedirect.com/topics/earth-and-planetary-sciences/bet-hedging>
32. Rosier, F. (2024, July 16). Widespread soil degradation alarms UNESCO. *Le Monde*. https://www.lemonde.fr/en/environment/article/2024/07/16/widespread-soil-degradation-alarms-unesco_6685619_114.html
33. Zentide. (2025, January 22). The impact of chemical fertilizer overuse on soil quality and climate change. Zentide. <https://zentide.co/blog/the-impact-of-chemical-fertilizer-overuse-on-soil-quality-and-climate-change/>
34. Kilic, T., & Bali, E. B. (2023). Biofilm control strategies in the light of biofilm-forming microorganisms. *World Journal of Microbiology & Biotechnology*, 39(5). <https://doi.org/10.1007/s11274-023-03584-6>
35. Natural Resources Conservation Service. (2022, November). Soil health: pH guide [PDF]. U.S. Department of Agriculture. https://www.nrcs.usda.gov/sites/default/files/2022-11/pH%20-%20Soil%20Health%20Guide_0.pdf
36. ScienceDirect Topics. (n.d.). Cyclic voltammetry – an overview. ScienceDirect. <https://www.sciencedirect.com/topics/materials-science/cyclic-voltammetry>